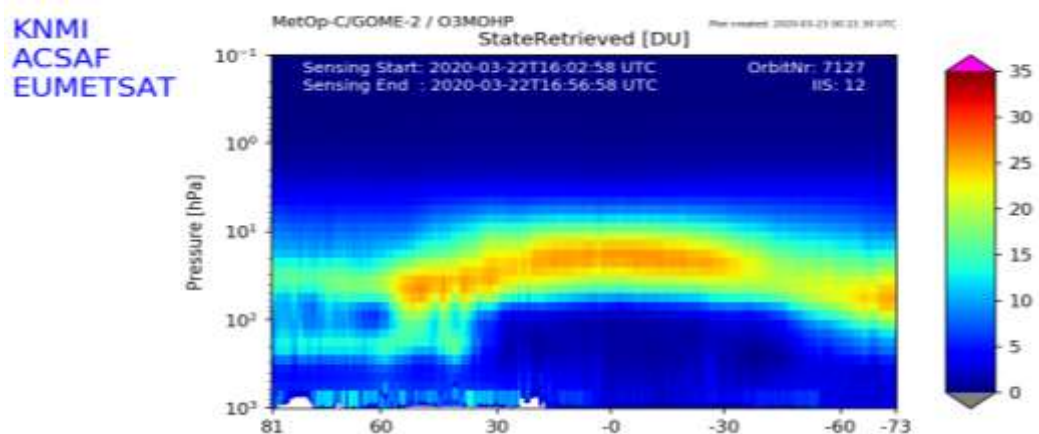


SAF/AC VALIDATION REPORT

Validated products:

Identifier	Name	Acronym
O3M-311	Near-Real-Time High Resolution Ozone Profile	NOP/HR
O3M-312	Offline High Resolution Ozone Profile	OOP/HR



Authors:

Name	Institute
Andy Delcloo	RMI
Katerina Garane	AUTH
Peggy Achtert	DWD

Reporting period:

February 2019 – December 2019

Validation methods:

Lidars and microwave radiometers (altitude range 15 – 60 km)

Balloon soundings (altitude range 0 – 34 km)

Dobson and Brewer observations (total column DU)

Input data versions:

Base Algorithm Version:6.3

Data processor versions:

Product Algorithm Version: 1.22

Product Software Version:2.07

Table of Contents

Introduction to EUMETSAT Satellite Application Facility on Atmospheric Composition monitoring (AC SAF).....	4
Applicable AC SAF Documents	5
Acronyms and abbreviations	6
1. General Introduction	7
2. Validation of ozone profiles using ozonesondes.....	7
2.1 Introduction	7
2.2 Dataset description	8
2.3 Comparison procedure	11
2.3.1 Co-location criteria.....	11
2.4 Ozone sounding pre-processing	11
2.5 Results	12
2.5.1 Difference profiles.....	12
2.6 Solar Zenith Angle dependency	17
2.7 Information content	18
2.8 General conclusions for the validation of ozone profiles, using ozonesondes.....	22
3. Validation of ozone profiles with lidar and microwave instruments	22
3.1 Instruments	22
3.2 Dataset description	23
3.3 Comparison procedure	25
3.4 Co-location criteria in time and space.....	25
3.5 Pre-processing of the ozone profiles.	26
3.6 Results	28
4. GOME-2/MetOp-C ozone integrated profiles validation using ground-based measurements	36
4.1 Dataset description	36
4.1.1 GOME-2/MetOp-C data.....	36
4.1.2 Ground-based data.....	36
4.1.3 GOME2/MetOp-A and GOME2/MetOp-B data.....	39
4.2 Validation of GOME-2C integrated ozone profiles	39
4.3 Conclusions from the GOME-2C integrated ozone profile validation	44

5. Acknowledgement.....	46
6. References	47
7. APPENDIX I.....	49

Introduction to EUMETSAT Satellite Application Facility on Atmospheric Composition monitoring (AC SAF)

Background

The monitoring of atmospheric chemistry is essential due to several human-caused changes in the atmosphere, like global warming, loss of stratospheric ozone, increasing UV radiation, and pollution. Furthermore, the monitoring is used to react to threats caused by natural hazards as well as to follow up the effects of international protocols.

Therefore, monitoring the chemical composition of the atmosphere and its effect on the Earth's radiative balance is a very important duty for EUMETSAT. The target is to provide information for policy makers, scientists and the general public.

Objectives

The main objectives of the AC SAF is to process, archive, validate and disseminate atmospheric composition products (O_3 , NO_2 , SO_2 , BrO, HCHO, H_2O , OClO, CO, NH_3), aerosol products and surface ultraviolet radiation products. The majority of the AC SAF products are based on data from the GOME-2 and IASI instruments onboard *EUMETSAT's* MetOp satellites.

Another important task besides the near real-time (NRT) and offline data dissemination is the provision of long-term, high-quality atmospheric composition products resulting from reprocessing activities.

Product categories, timeliness and dissemination

NRT products are available in less than three hours after measurement. These products are disseminated via EUMETCast, WMO GTS or the internet.

- Near real-time trace gas column (total and tropospheric O_3 and NO_2 , total SO_2 , total HCHO, CO) and high-resolution ozone profile
- Near real-time absorbing aerosol index (AAI) from main science channels and polarization measurement detectors
- Near real-time UV index, clear-sky and cloud-corrected

Offline products are available within two weeks after measurement and disseminated via dedicated web services at EUMETSAT and AC SAF.

- Offline trace gas column (total and tropospheric O_3 and NO_2 , total SO_2 , total BrO, total HCHO, total H_2O) and high-resolution ozone profile
- Offline absorbing aerosol index from main science channels and polarization measurement detectors
- Offline surface UV, daily doses and daily maximum values with several weighting functions

Data records are available after reprocessing activities from the EUMETSAT Data Centre and/or the AC SAF archives.

- Data records generated in reprocessing
- Lambertian-equivalent reflectivity
- Total OCIO

Users can access the AC SAF offline products and data records free of charge by registering at the AC SAF web site.

More information about the AC SAF project, products and services: <https://acsaf.org/>

AC SAF Helpdesk: helpdesk@acsaf.org

Twitter: https://twitter.com/Atmospheric_SAF

Applicable AC SAF Documents

[ATBD] Algorithm Theoretical Basis Document for Near Real Time and Offline Ozone profiles, KNMI/GOME/ATBD/01/001, issue 2.0.1, Olaf Tuinder, 20181115.

[PUM] Product User Manual for Near Real Time and Offline Ozone profiles, KNMI/GOME/PUM/001, issue 2.00, Olaf Tuinder, 20181115.

Both documents are available at <http://acsaf.fmi.fi> in the *Documents* section.

Acronyms and abbreviations

ATBD	Algorithm Theoretical Basis Document
AUTH	Aristotle University of Thessaloniki
DOAS	Differential Optical Absorption Spectroscopy
GAW	Global Atmosphere Watch
GDP	GOME Data Processor
GOME	Global Ozone Monitoring Experiment
LAP/AUTH	Laboratory of Atmospheric Physics/Aristotle University of Thessaloniki
MetOp	Meteorological Operational satellite
MWR	Microwave Radiometers
NDACC	Network for the Detection of Atmospheric Composition Change
NH	Northern Hemisphere
O3-CCI	Ozone – Climate Change Initiative
OMI	Ozone Monitoring Instrument
OPERA	Ozone Profile Retrieval Algorithm
SH	Southern Hemisphere
SZA	Solar Zenith Angle
TOC	Total Ozone Column
TOMS	Total Ozone Mapping Spectrometer
TrOC	Tropospheric integrated Ozone Column
WMO	World Meteorological Organization
WOUDC	World Ozone and UV Data Center

1. General Introduction

This report contains validation results of the GOME-2/MetOp-C ozone profile product, retrieved by the Ozone Profile Retrieval Algorithm (OPERA) at KNMI. It covers the time period from February 2019 to December 2019. Ozone profiles retrieved from processed level-1b data were retrieved with 80 km x 40 km resolution.

Since this work was carried out in three different institutions, this document is split up into three separate parts. The first part contains the validation of the retrieved GOME-2 ozone profiles using ozonesondes (chapter 2). This part validates the retrieved ozone profiles in the troposphere and the lower stratosphere. The second part (chapter 3) uses measurements with lidars and microwave radiometers to assess the performance of GOME-2 ozone profiles; primarily in the stratosphere from 20 to 60 km altitude. The third part of this report (chapter 4), covers the validation of the integrated ozone profile product through an intercomparison with ground truth data from spectrophotometers (Dobson and Brewer). Additionally, the consistency of the integrated ozone profile of GOME-2/MetOp-C is examined by intercomparison to the respective products from GOME-2/MetOp-B and -A, as well as the official TOC product of GOME-2/MetOp-C processed with the GDP4.9 algorithm. This work is done by AUTH. The outcome of the different validation parts is summarized in the summary and conclusions section at the end of this report.

Tabel 1.1 presents the different accuracies which are taken into account to assess the quality of the product.

Tabel 1.1: Different intended accuracies for ozone profiles, provided in the Product Requirements Document SAF/AC/FMI/RQ/PRD/001

Accuracy		
Threshold	Target	Optimal
30 % in stratosphere	15 % in stratosphere	10 % in stratosphere
70 % in troposphere	30 % in troposphere	25 % in troposphere

2. Validation of ozone profiles using ozonesondes

2.1 Introduction

This report presents validation results for the AC SAF GOME-2 ozone profile product. The validation was carried out using ozone sounding profiles.

Ozonesondes are lightweight balloon-borne instruments which measure ozone concentrations from the surface up to about 30 km with much better vertical resolution than possible from

satellite data. In general, measurement precision and accuracy are also better compared to satellite observations, at least in the lower stratosphere and the troposphere. Another advantage is that ozone soundings can be performed at any time and during any meteorological condition.

The precision of ozonesondes varies with altitude and depends on the type of ozonesonde used. Tabel 2.1 shows indicative precision of the Electrochemical Concentration Cell (ECC) and Brewer-Mast (B-M) ozonesondes at different pressure levels of the sounding.

Tabel 2.1: Precision (in percent) of different types of ozonesondes at different pressure levels.

Pressure level (hPa)	ECC	B-M
10	2	10
40	2	4
100	4	6
400	6	16
900	7	14

Profiles from ozonesondes are most reliable around the 40 hPa level, which is around the ozone maximum. The error bar of profiles from ozonesondes increases rapidly at levels above the 10 hPa level, which is at around 31 km altitude. For this validation report, only the station of Hohenpeissenberg is using B-M sondes. The other stations under consideration (Table A. 3) use ECC sondes.

2.2 Dataset description

GOME-2 ozone data used in this validation report covers the time period from February 2019 to December 2019. GOME-2 ozone data was made available by KNMI at pre-selected site where ozone soundings are performed on a regular basis. Data was made available by the World Ozone and Ultraviolet Data Center (WOUDC). (<http://www.woudc.org>) and the NILU's Atmospheric Database for Interactive Retrieval (NADIR) at Norsk Institutt for Luftforskning (NILU) (<http://www.nilu.no/nadir/>). In Figure 2.1, an overview is shown from the ozonesonde station data used in this report.

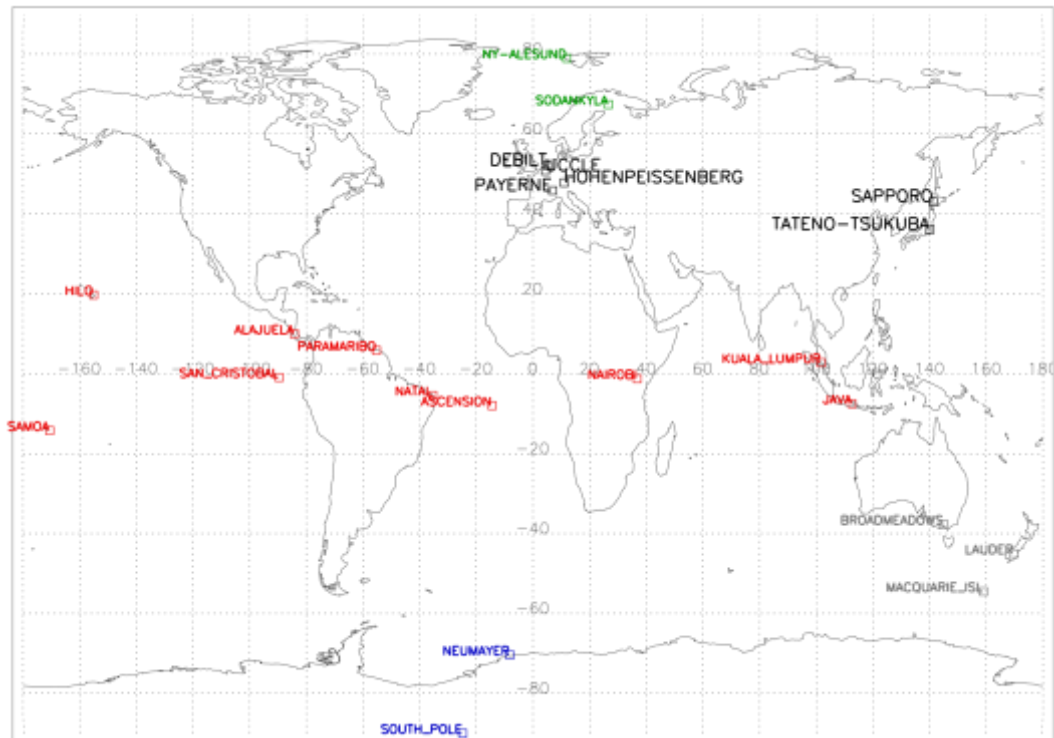


Figure 2.1: Stations consulted for validation. Latitude belts from north to south: polar stations north: green (67N – 90 N), midlatitude stations north: black (30 N – 67 N), Tropical stations: red (30 N – 30 S), midlatitude stations south: grey (30 S – 70 S), polar stations south: blue (70 S – 90 S).

The timeline of the vertically integrated GOME-2C ozone profile is presented in Figure 2.2. More information and images for the other sensors are available at:

<http://www.temis.nl/o3msaf/timeseries.php?sat=metopa>

<http://www.temis.nl/o3msaf/timeseries.php?sat=metoph>

<http://www.temis.nl/o3msaf/timeseries.php?sat=metopc>

Ozonesonde data are generally made available by the organization carrying out observations after a short delay related to data quality assurance. Nevertheless, some organizations make their ozone profile data readily available for validation purposes. The time period we consider here for the validation of MetOp-C is from February 2019 to December 2019.

Table A. 3 of the Appendix shows an overview of the station data used in this validation report using ozonesondes and the collocations in space and time are shown in Figure 2.3.

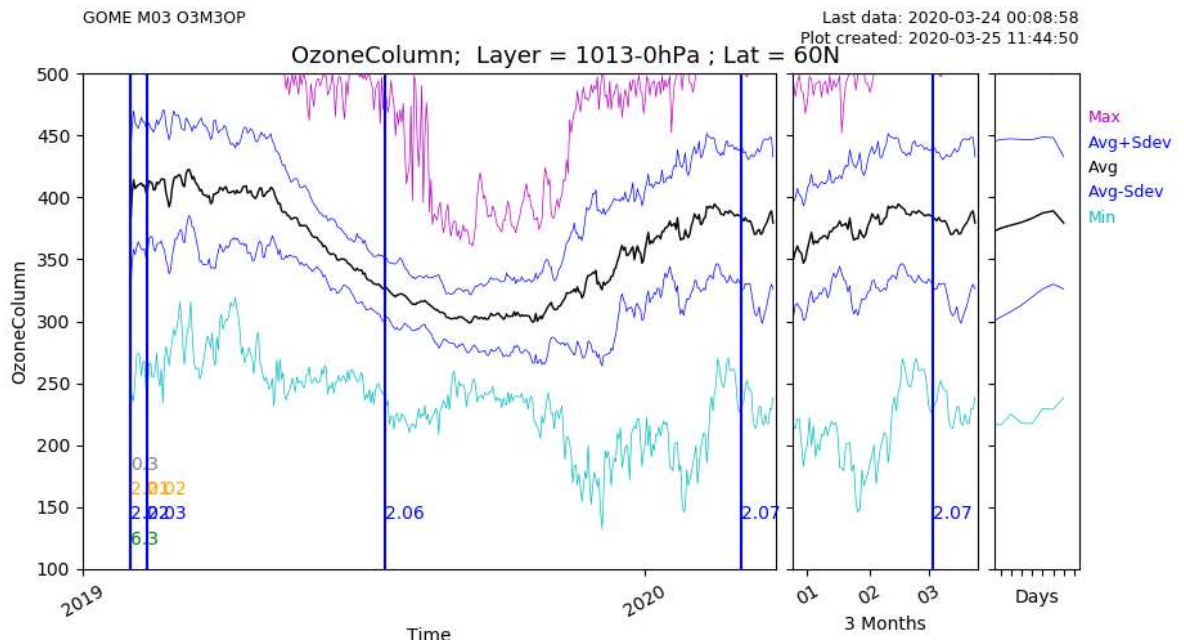


Figure 2.2: Timeline of vertically integrated Metop-C ozone profiles (=total ozone columns) and changes in data processor (vertical lines). The coloured lines refer to PPF version (green), Software version PGE (blue), Algorithm version (orange) and Config version.

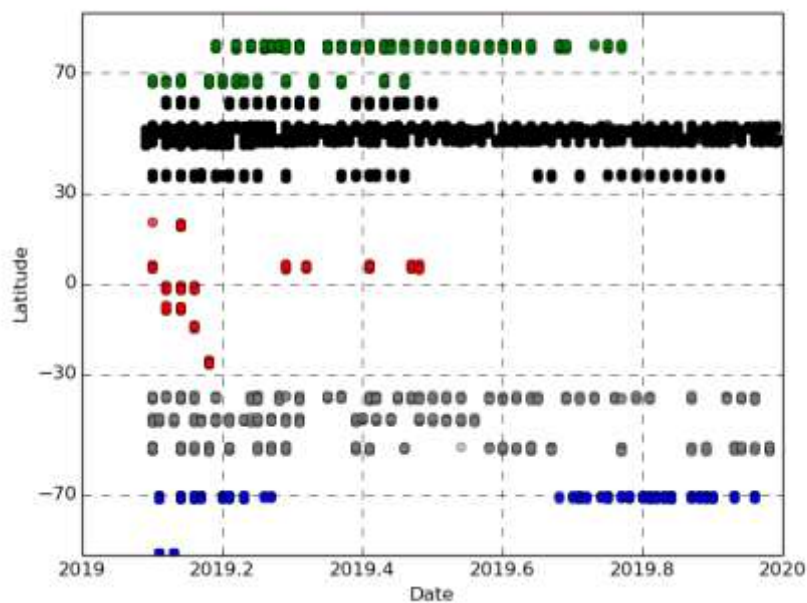


Figure 2.3: Spatial and temporal representation of the collocation data used for the validation with ozonesonde data for the time period from February 2019 to December 2019.

2.3 Comparison procedure

2.3.1 Co-location criteria

The selection criteria are twofold:

- The geographic distance between the GOME-2 pixel center and the sounding station location is less than 100 km.
- The time difference between the pixel sensing time and the sounding launch time is less than ten hours.

Each sounding that is correlated with a GOME-2 overpass is generally correlated with several GOME-2 pixels if the orbit falls within this 100 km circle around the sounding station. This means that a single ozone profile is compared to more than one GOME-2 measurement.

2.4 Ozone sounding pre-processing

GOME-2 ozone profiles are given as partial ozone columns on 40 varying pressure levels calculated by the Ozone Profile Retrieval Algorithm (OPERA) developed by KNMI. Ozone partial columns are expressed in Dobson Units.

Ozonesondes measure ozone concentration along the ascent with a typical vertical resolution of 100 m while GOME-2 profiles consist 40 layers between the ground and 0.001 hPa. Ozonesondes give ozone concentration in partial pressure. The integration requires interpolation, as GOME-2 levels never match exactly ozonesonde layers. This interpolation causes negligible errors given the high vertical resolution of ozonesonde profiles.

For comparison, ozonesonde profiles are integrated between the GOME-2 pressure levels. When a single ozonesonde profile is compared to different GOME-2 profiles, the actual reference ozone values are not the same given that the GOME-2 level boundaries vary from one measurement to another. Integrated ozonesondes data will be referred to in this report as X_{sonde} .

GOME-2 layers are relatively thick and GOME-2 layer boundaries show small variations compared to the layer thickness. Hence, individual layers generally occur around the same altitude. The altitude of those layers can be considered as “fixed” and therefore the center of an “*averaged layer altitude (or pressure)*” is used in plotting the data.

In this report, the validation of the GOME-2 profiles is calculated by using the averaging kernels (AVK) of the GOME-2 profile. The motivation to apply the AVK is to “smooth” the ozone soundings towards the resolution of the satellite:

$$X_{\text{avk_sonde}} = X_{\text{apriori}} + A (X_{\text{raw sonde}} - X_{\text{apriori}}) \quad (1)$$

Where A represents the averaging kernel, $X_{\text{avk_sonde}}$ is the retrieved ozone sonde profile, X_{sonde} is the ozone sonde profile and X_{apriori} is the a priori profile.

2.5 Results

2.5.1 Difference profiles

The relative difference between the ozone profiles from GOME-2 and an ozonesonde is calculated as:

$$(X_{\text{GOME-2}} - X_{\text{sonde}})/X_{\text{sonde}} \quad (2)$$

For comparing the GOME-2 ozone profile with the smoothed ozonesonde profiles (AVK ozonesondes) the following equation is used:

$$(X_{\text{GOME-2}} - X_{\text{AVK-SONDE}})/X_{\text{AVK-SONDE}} \quad (3)$$

Figure 2.4 shows relative difference profiles between GOME-2 ozone profiles at the one hand and on the other hand ozonesonde-, and AVK ozonesonde profiles for different latitude belts and using different types of ozonesondes, listed in Tabel 2.1.

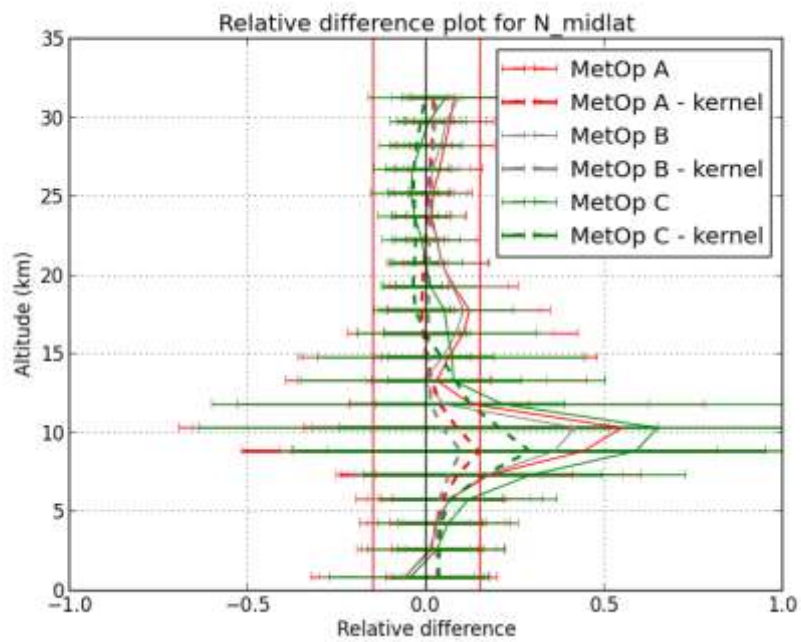
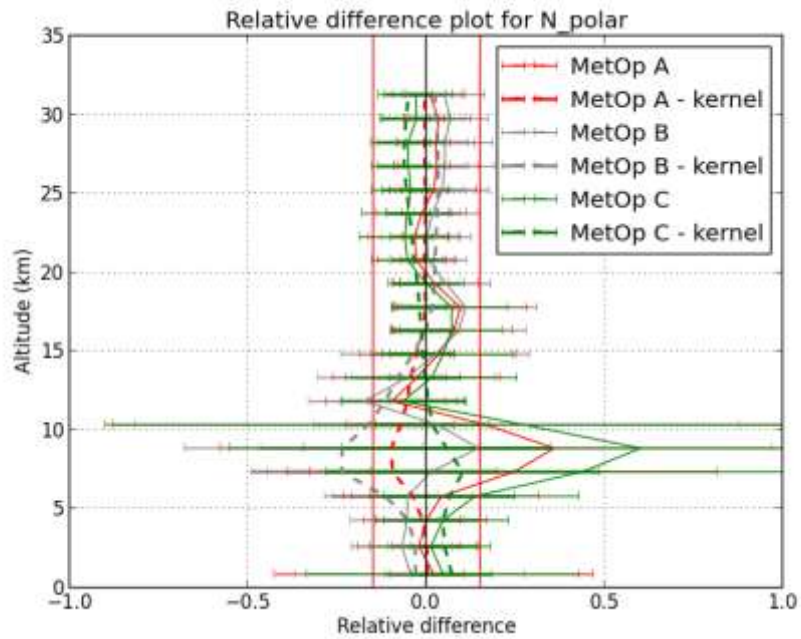
Please note that we don't yet have a full year of data available for this validation effort. In this subsection, we will first describe the statistics for the considered time period February 2019 – December 2019 and compare it with the operational results of MetOp-B (time period January 2019 – December 2019). In the next sections, we will discuss the seasonal behavior and other possible influences on the quality of the ozone profile product.

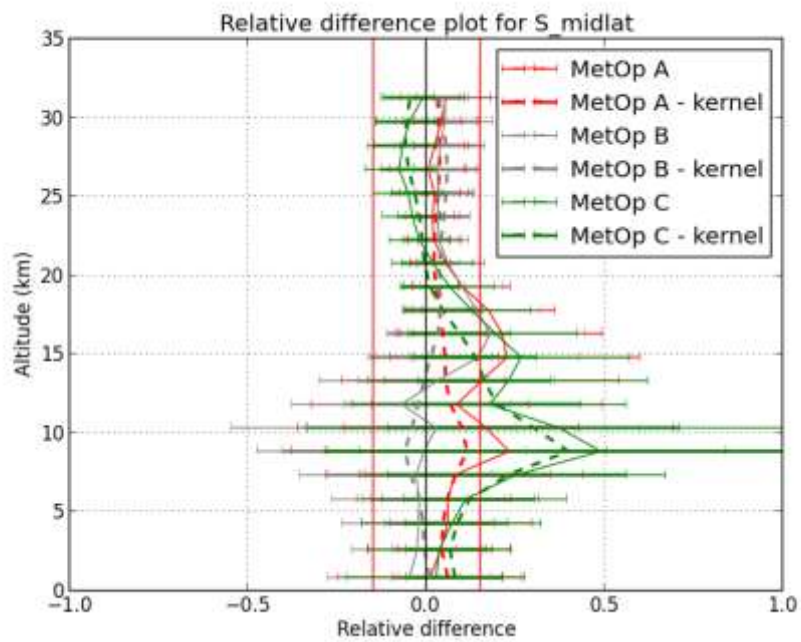
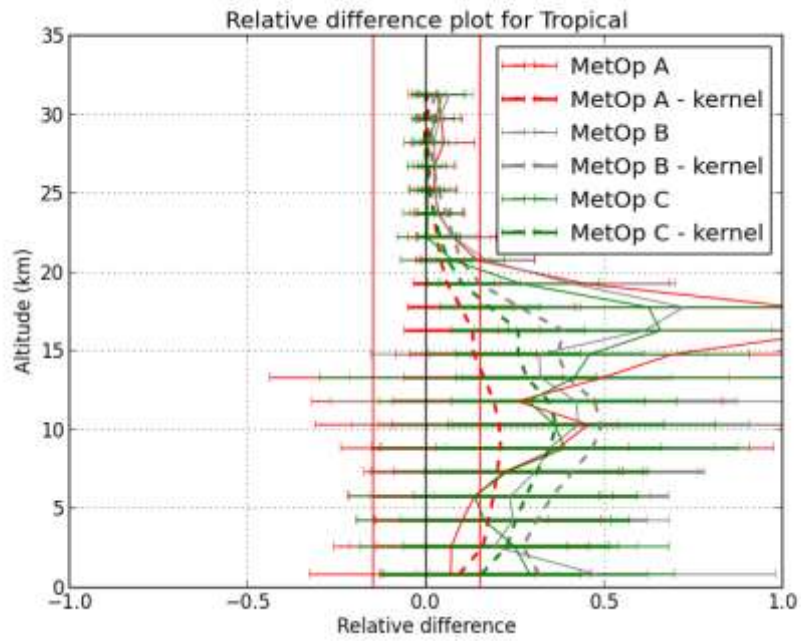
For the polar and midlatitude stations, the difference plots in Figure 2.4 show that GOME-2 ozone profiles are within the target error range of 15% compared to the ozonesonde reference, except for the Upper Troposphere – Low Stratosphere (UTLS) region. For the lower troposphere, most of the latitude belts show relative differences within 15%. Applying the averaging kernels improves the comparison significantly. For the tropical stations, there is a significant overestimation of tropospheric ozone, but the statistics are within the threshold value of 50%.

These results show that the statistics for the new GOME-2C ozone profile product compared to GOME-2B and GOME-2A show similar behaviour, with in general obtaining better results for the new sensor GOME-2C which are closer to the target values (Tabel 1.1) for the different height ranges under consideration.

Since tropospheric integrated ozone column (TrOC) is an official operational product, its results are not mentioned in this report. Here we will focus on the quality of the ozone profiles and the way we communicate the results in the two-yearly operational reports. These documents are available at <http://acsaf.fmi.org> in the *Documents* section ([operational reports](#)).

Table 2.1 provides an overview of the height ranges related to the troposphere, the UTLS-zone and the stratosphere.





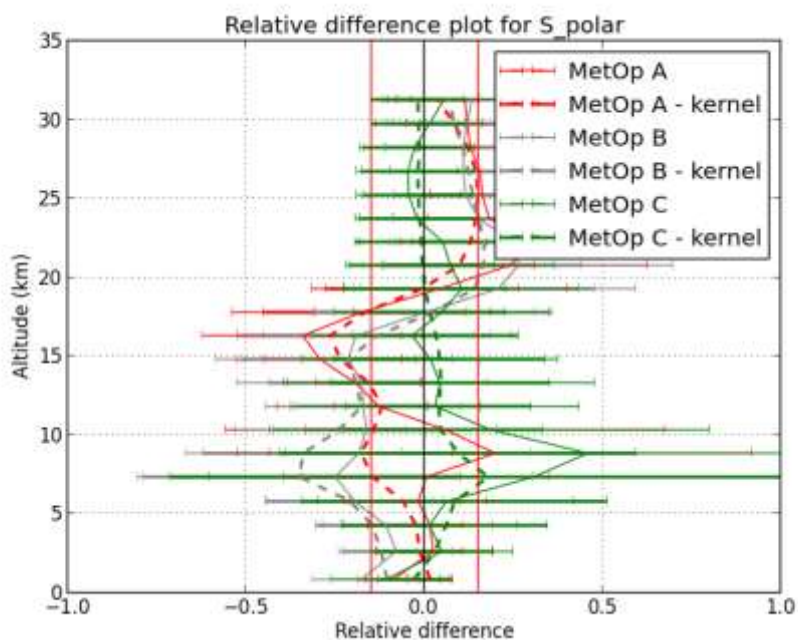


Figure 2.4: Relative difference in ozone profiles from GOME-2, ozonesondes and smoothed ozonesondes according to equations (2) and (3) for different latitude belts and for different sensors (GOME-2A/2B/2C) for the time period February 2019 to December 2019 (GOME-2C) and for the time period January 2019 to December 2019 for GOME-2A/2B. The error bars represent one standard deviation on the mean error.

Table 2.1: Definition of the ranges in km for troposphere, UTLS-zone and stratosphere for the different latitude belts.

	Troposphere	UTLS	Stratosphere
Polar Regions	< 6 km	6 km - 12 km	12 km - 30 km
Mid-Latitudes	< 8 km	8 km - 14 km	14 km - 30 km
Tropical Regions	< 12 km	12 km - 18 km	18 km - 30 km

Table 2.2: Relative Differences (RD) and standard deviation (STDEV) of GOME-2 ozone profiles product with respect to XAVK-sonde for the lower stratosphere for the five latitude belts under consideration for the time period from February 2019 to December 2019.

Lower Stratosphere			
February 2019 - December 2019	AD (DU)	RD (%)	STDEV (%)
northern polar region	-8.2	-3.6	7.3
northern midlatitudes	-5.8	-2.2	8.4
tropical regions	2.9	2.7	4.8
southern midlatitudes	-2.0	0.5	9.0
southern polar region	0.0	0.4	20.2

*The relative difference statistics are derived as a weighted average over the lower- and upper stratospheric ozone profile levels. The absolute differences however are integrated over respectively the lower- and upper stratospheric ozone profile levels.

Table 2.2 shows an overview of the obtained results for the time period from February 2019 to December 2019 for the lower stratosphere.

For the ozone profile product, also the optimal values are met in the lower stratosphere. This is not taking into account the UTLS-zone, which shows more elevated relative differences that cannot be appointed to the troposphere or the stratosphere. The results for the troposphere are shown in the validation report on tropospheric ozone column products from GOME-2C ozone profile products, available at <https://acsaf.org> in the documents section ([validation reports](#)).

2.6 Solar Zenith Angle dependency

Previous studies with GOME-2/MetOp-A data (Delcloo and Kreger, 2013) have shown that the GOME-2 ozone profile retrieval shows a seasonal dependency and is also influenced by the Solar Zenith Angle (SZA). Figure 2.5 and Figure 2.6 show the dependency on SZA for the northern midlatitude and the northern polar stations for GOME-2C. Especially for the high ozone concentrations around 22-23 km in altitude (location of the ozone maximum), a seasonal behavior is present.

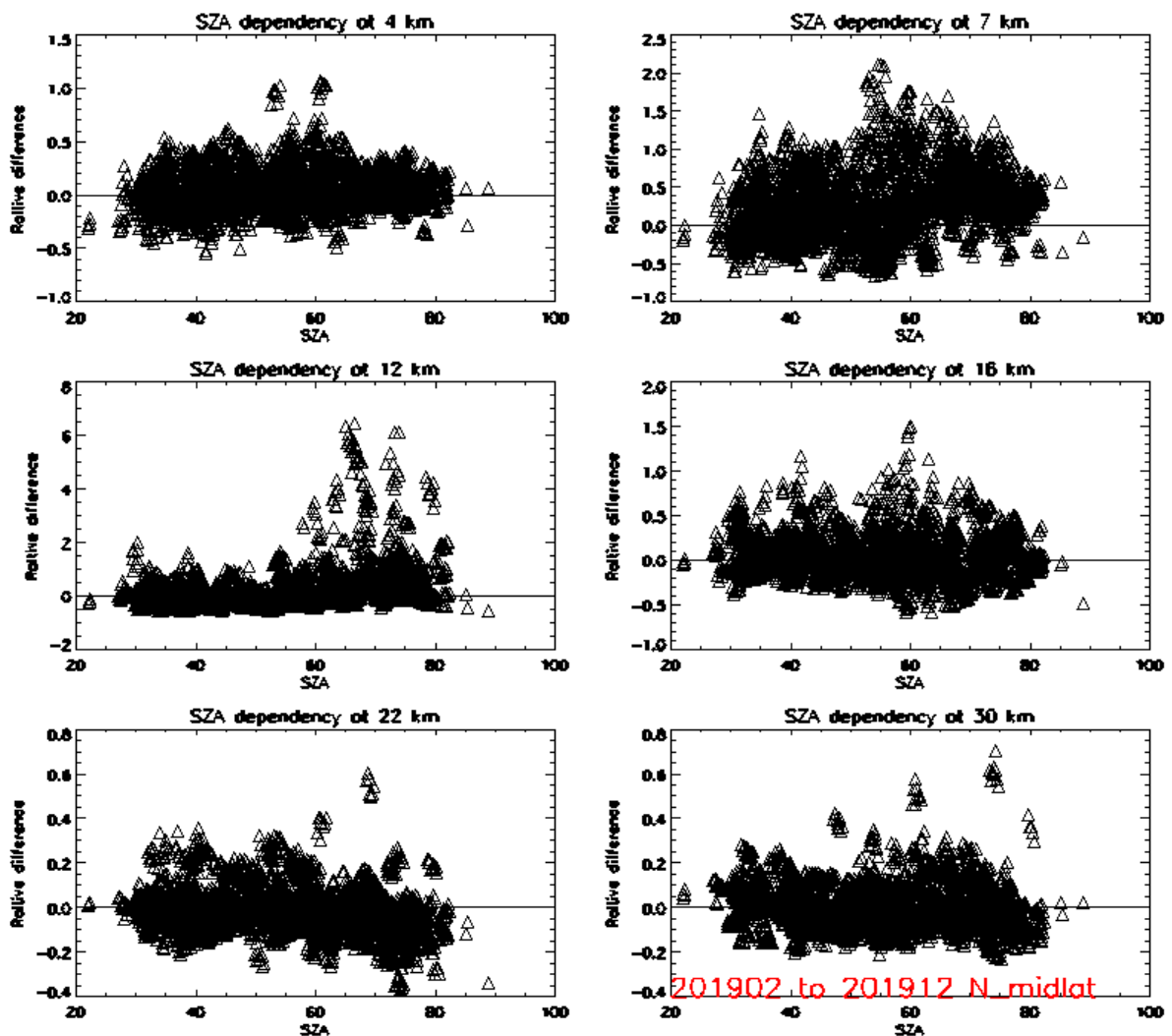


Figure 2.5: Solar Zenith Angle dependency at six altitude levels for the northern midlatitude stations, time period February 2019 – December 2019

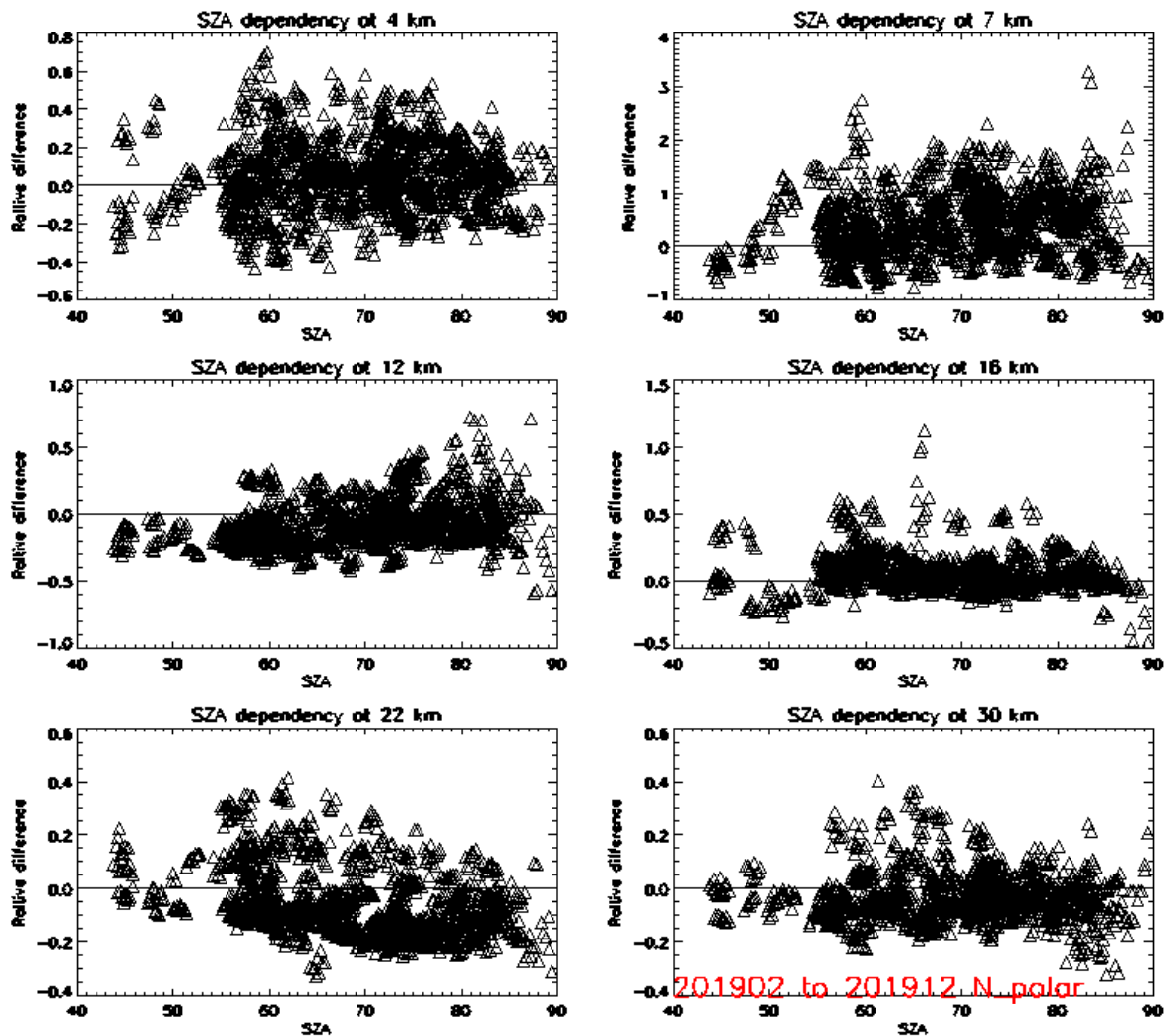


Figure 2.6: Solar Zenith Angle dependency for six altitude levels for the northern polar stations, time period February 2019 – December 2019

2.7 Information content

Scatter plots, showing the retrieved ozone partial columns as a function of the reference partial column measured by ozonesondes give a measure of the amount of information actually present in the retrieved layer. This is shown in Figure 2.7 for the northern midlatitude stations at six different altitude levels. The slope of the regression line can be seen as a measure for the amount of information actually present in the retrieved layer. To show the influence of applying the averaging kernels it is shown from Figure 2.8 that the slope values are improved (closer to 1) while the intercept values are closer to 0.

The interpretation of “better results” should be taken with care. Applying the kernels using equation 1 is a way to smooth the ozone profile towards a comparable vertical resolution of the retrieved ozone profile. High resolution effects like filaments present for example in secondary ozone maxima are mostly not seen by GOME-2 which results in sometimes large differences between observed and retrieved partial ozone columns.

The regression line in the scatter plots show that GOME-2 loses sensitivity in the lower troposphere and around the UTLS-zone (Figure 2.7).

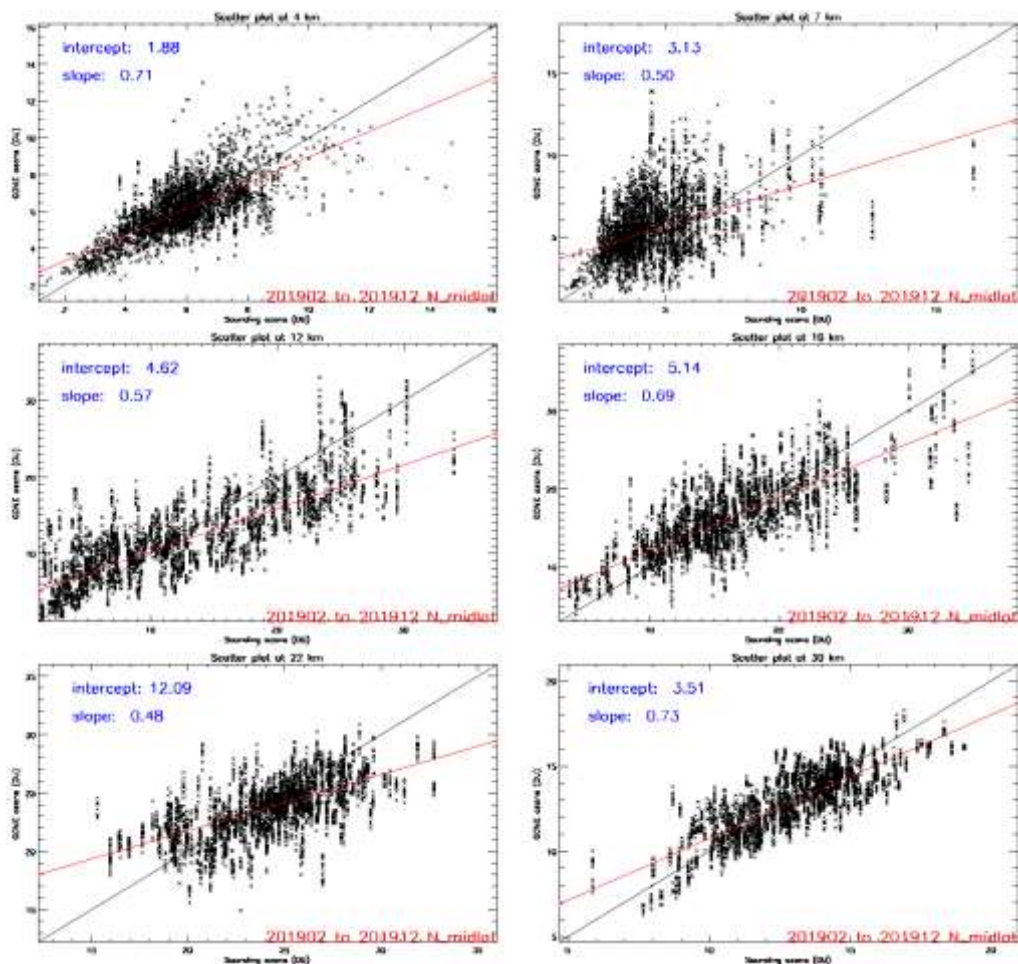


Figure 2.7: Scatter plot at 6 different altitude levels for the stations at northern midlatitudes (February 2019- December 2019).

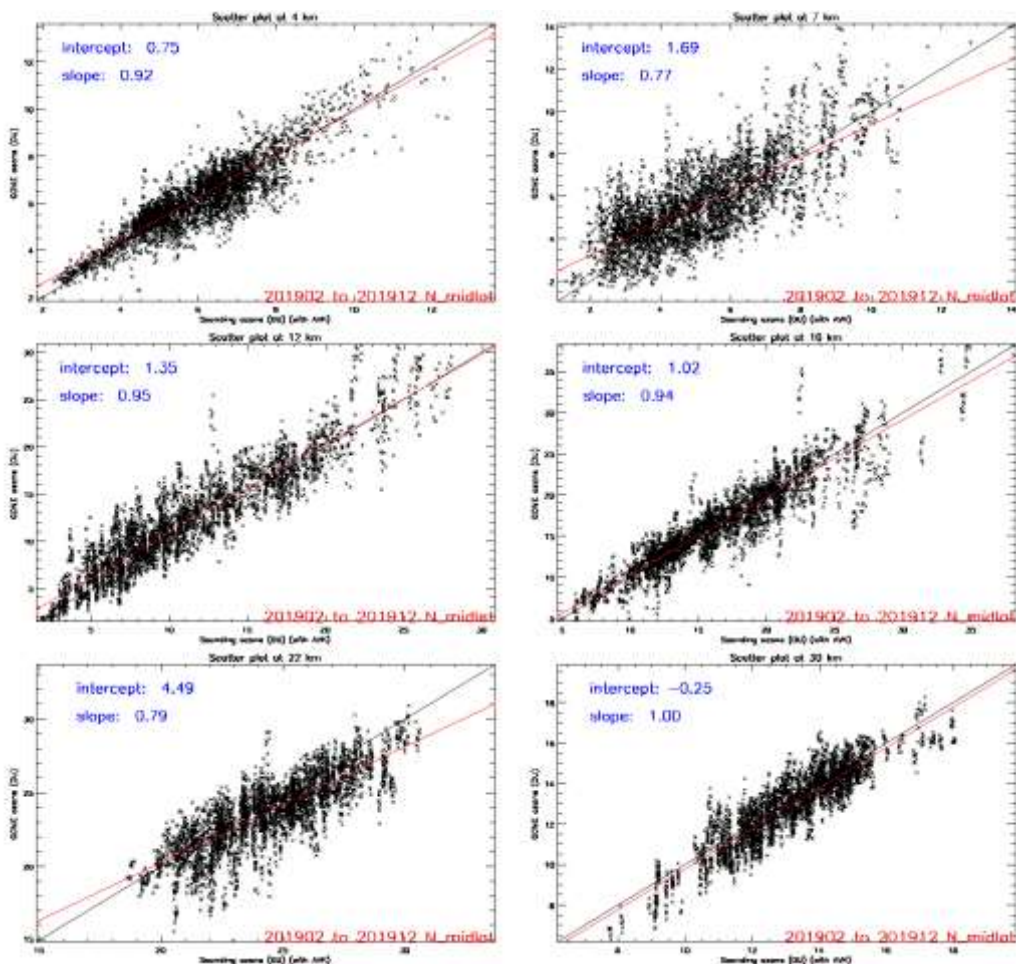


Figure 2.8: Scatter plot at 6 different altitude levels for the stations at northern midlatitudes (February 2019- December 2019), applying the kernels

Besides the influence on SZA, the dependence on cloud cover, seasonal behaviour has been verified. For cloud cover, we could not pinpoint any specific dependence on cloud cover. For the seasonal behaviour, it is known from previous reports (Delcloo and Kreher, 2013) that there is some seasonal behaviour present. This is especially true for the lower altitudes and can be seen in the Figure 2.9 for northern midlatitude stations. More results can be consulted on the [official validation website for ozone profiles](#): when this product is declared operational.

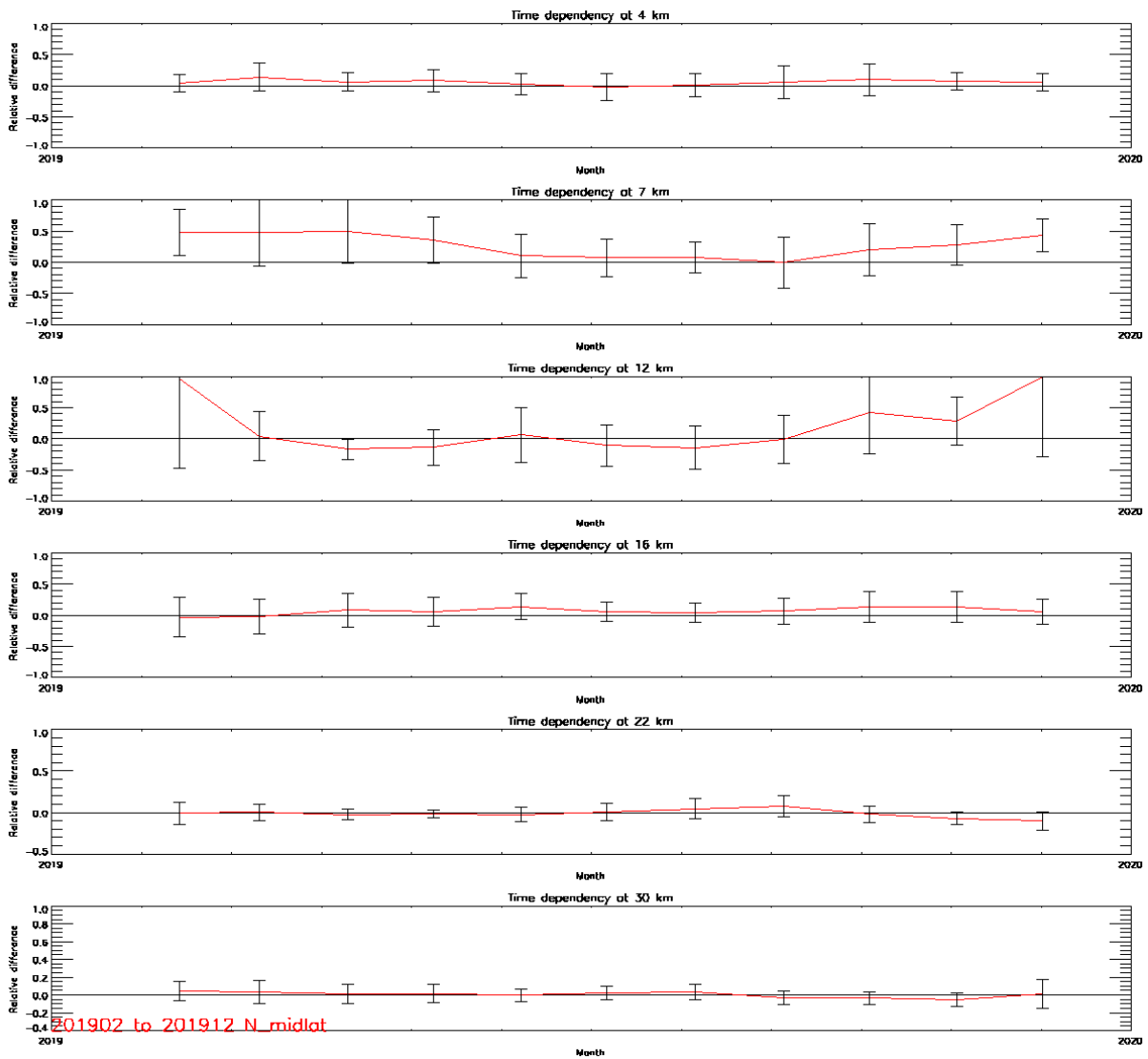


Figure 2.9: Time series at 6 different altitude levels for the stations at northern midlatitudes (February 2019 - December 2019)

2.8 General conclusions for the validation of ozone profiles, using ozonesondes

The GOME-2C vertical ozone profile product was validated using ozonesonde data and have been compared with the ozone profile product onboard GOME-2A and GOME-2B. The validation results have revealed the following properties:

- The comparisons of all three sensors show comparable results and are all within target value for the lower stratosphere.
- GOME-2 ozone profile retrieval shows a Solar Zenith Angle (SZA) dependency, especially for the altitude range 20 – 25 km (region where the ozone maximum is located).
- Besides the influence on SZA, the dependency on cloud cover and seasonal behaviour has been verified. For cloud cover, we could not pinpoint any specific dependency. For the seasonal behaviour, this dependency is true for the lower altitudes of the ozone profile.

It is shown that the optimal value (10% accuracy) is met in the lower stratosphere (Table 2.3) for all belts under consideration.

3. Validation of ozone profiles with lidar and microwave instruments

3.1 Instruments

Lidars and microwave radiometers (MWR) are the main ground-based instruments available for validation purposes in the upper stratosphere. Their altitude range covers typically 15 km to 50 or 60 km (Table 3.1). This significantly extends the range covered by ozonesondes towards higher altitudes. It also provides a good overlap from 15 to 30 km altitude. Note that there are only about 10 operational lidar and MWR stations on the globe that provide regular data, though not as rapidly and operationally as the ozonesonde stations. Typically, ozone profiles do not become available until several weeks after the measurement.

The Differential Absorption Lidar (DIAL) technique provides accurate vertical profiles of ozone in the altitude range from 15 to 50 km, depending on the individual lidar system (Godin et al., 1989). Clouds and daylight conditions inhibit good measurements (Leblanc and McDermid, 2000; Steinbrecht et al., 2006), so lidar ozone profiles are restricted to cloud free nights. Typically, 5 to 8 lidar measurements per month are taken at a station. Depending on atmospheric conditions and lidar system efficiency, each ozone profile measurement covers several hours. For the lidars, number density versus geometric altitude is the natural coordinate system of the measurement.

MWR measures the thermal radiation of a pressure broadened emission line. Line-shape depends on the pressure/ altitude profile of ozone (Lobsiger et al., 1984; Parrish et al., 1988). Measurement of the precise line-shape, thus, allows for retrieving the ozone profile. Similar to many satellite measurements, an optimal estimation retrieval (Rodgers, 1990) provides ozone profiles in various coordinate systems, including number density versus altitude for the NDACC MWR profiles. MWR ozone profiles typically cover 20 to 60 km altitude. In contrast to lidars, MWR has little weather dependence, and measures during daylight as well. On average, MWR profiles are measured on 20 days per month. The integration time of one MWR profile varies from 30 minutes to 5 hours, depending on the individual instrument (Boyd et al., 2007; Hocke et al., 2007).

Table 3.1: Typical precision and height resolution of lidars and MWR (Steinbrecht et al., 2006)

lidar		microwave radiometer		
Height [km]	Precision [%]	height resolution [km]	precision [%]	height resolution [km]
15	5	1.4		
20	5	1.2	3	10
25	3	1.0	3	10
30	3	1.8	3	10
35	3	4.2	3	14
40	5	7.2	3	14
45	15	8.6	3	20
50	55	8.6	3	20
50-70			3	20

3.2 Dataset description

The ground-based validation profiles come from the NDACC (Network for the Detection of Atmospheric Composition Change, <http://www.ndsc.ncep.noaa.gov/>). NDACC lidar and microwave instruments go through an evaluation process and thorough quality checks (Keckhut et al., 2004). The ozone profiles are not available in near real time. A minimum of one month is necessary before profiles become available but most stations need three or more months. NDACC demands that ozone profiles are submitted at least once per year to their database.

NDACC stations used for validation

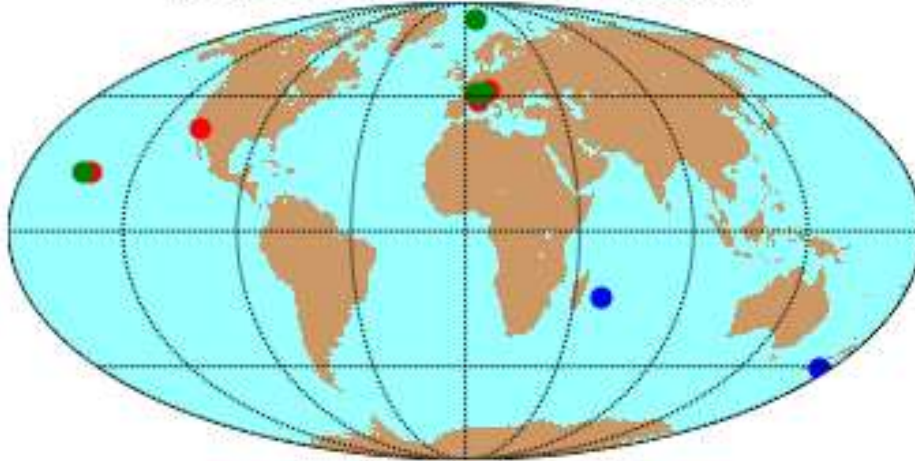


Figure 3.1: Stations consulted for validation. Lidar station in red and microwave station in green. The blue stations could not be used in this validation report.

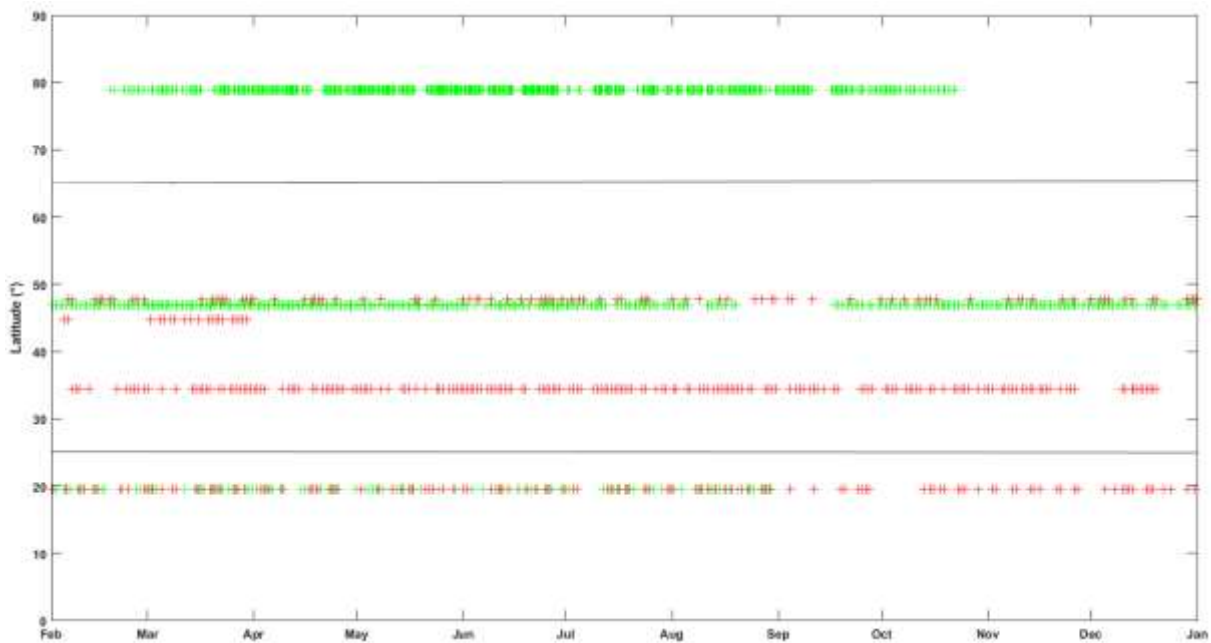


Figure 3.2: Spatial and temporal representation of the collocation data used for the validation with lidar (red) and microwave data (green) for the time period from February 2019 to December 2019.

The stations (Figure 3.1) used in this validation for the lidar/microwave data are the Network for the Detection of Atmospheric Composition Change (NDACC) stations at Ny-Ålesund (microwave, 78.92° N, 11.93° E), Hohenpeissenberg (lidar, 47.8° N, 11.0° E), Bern (microwave, 46.95° N, 7.45° E), Haute-Provence (lidar, 43.94° N, 5.71° E), Table Mountain (lidar, 34.4° N, 117.7° W), and Mauna Loa (lidar, 19.54° N, 155.58° W). The stations Reunion (lidar, 21.07° S, 55.39°E) and Lauder (lidar, 45.04° S, 169.68° E) could not be used for this validation, due to instruments problems and lack of data.

The collocations in space and time of the ground-based data are shown in Figure 3.2. Polar stations north are located between 65N and 90 N, the midlatitude stations north are between 25 N and 65 N, and the tropical stations are located between 25 N – 25 S.

3.3 Comparison procedure

Generally, the comparison procedure is the same as for the ozonesondes, outlined in Section 2 (see also Delcloo and Kins, 2009; 2012). Different temporal resolution and measurement frequency of the ground-based instruments, however, require some minor changes.

3.4 Co-location criteria in time and space

Only ground-based and satellite profiles that are close in space and in time to a GOME-2 profile are compared. Nightly mean lidar measurements are compared to GOME-2 profiles measured either the morning after or the morning before the lidar profile. This means that a maximum time difference of 20 hours is allowed.

MWR measure around the clock, typically one profile every hour. So usually MWR profiles can be compared with GOME-2 ozone profiles measured within less than 2 hours. Usually all GOME-2 measurements are made in the local morning.

Only GOME-2 profiles with ground pixels centers closer than 200 km to the validation stations were considered. A 200 km radius typically gives about 50 co-located GOME-2 high resolution profiles per station and per day. The number of coarse resolution profiles is lower, but still provides a good statistical basis. Larger co-location radii result in larger geophysical differences, smaller radii result in too few comparisons cases.

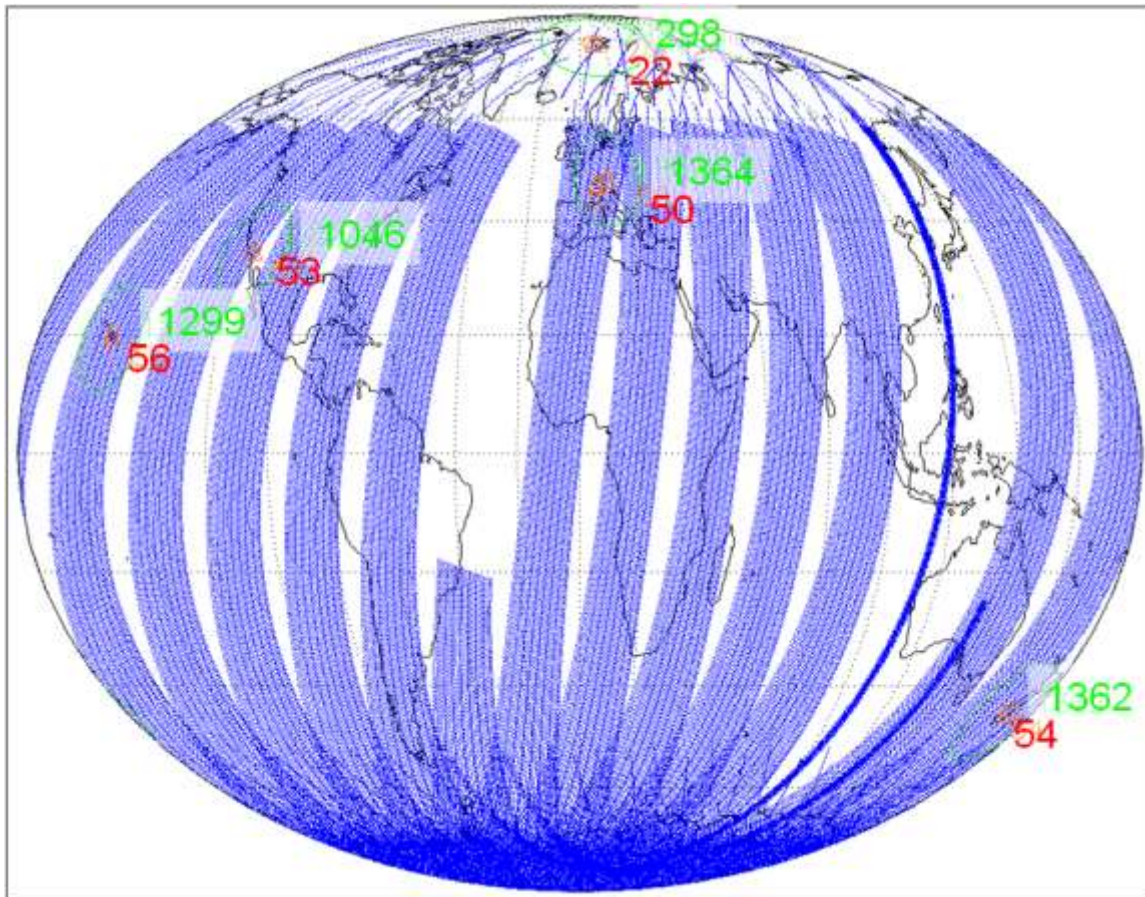


Figure 3.3: World map with GOME-2 high resolution ground pixels for Dec.17th, 2012. Red triangles show NDACC lidar and microwave stations. Green circles are for 1000 km radius around the station. Green numbers give the number of GOME-2 ground pixels within the 1000 km circle. Red circle and red numbers are for a 200 km radius. GOME-2 swaths start in the North near the date-line, and then move westwards around the globe. All measurements are taken in the local morning. Note that in December there is no sunlight near the North Pole, so there are no measurements there.

3.5 Pre-processing of the ozone profiles.

Like the ozonesonde data, lidar and MWR ozone number density profiles are first averaged over the GOME-2 retrieval layers, usually 40 layers, about 2 km wide. The resulting slightly smoothed profiles are called X_{ref} .

In the next step, the X_{ref} lidar and MWR profiles are further smoothed over altitude by applying the GOME-2 averaging kernels (with proper scaling). These smoothed profiles X_{AVK} have altitude resolution comparable to the GOME-2 profiles (or coarser).

Since the GOME-2 measurement alone does not fully constrain the retrieved ozone profile, GOME-2 profiles are a mix of measured information and a-priori “climatological” ozone

profiles. At altitudes where the measurement provides tight constraints, the retrieved ozone comes to 80% or 90% of the measurement. At other altitudes (usually the troposphere and mesosphere), the GOME-2 profile comes to 80% or 90% of an a-priori profile. For the validation of the retrieval process, it makes sense to also consider reference profiles that have been smoothed by the averaging kernels, and have the same mix of measured and a-priori profile as the GOME-2 profiles. Eq. 1 (see Section 2.3) describes the underlying mathematics. The resulting profiles are called $X_{AVK\ apriori}$ in the following.

In nearly all cases, the validation of GOME-2 profiles gives almost the same results for the three version of smoothed reference profiles X_{ref} , X_{AVK} , and $X_{AVK\ apriori}$.

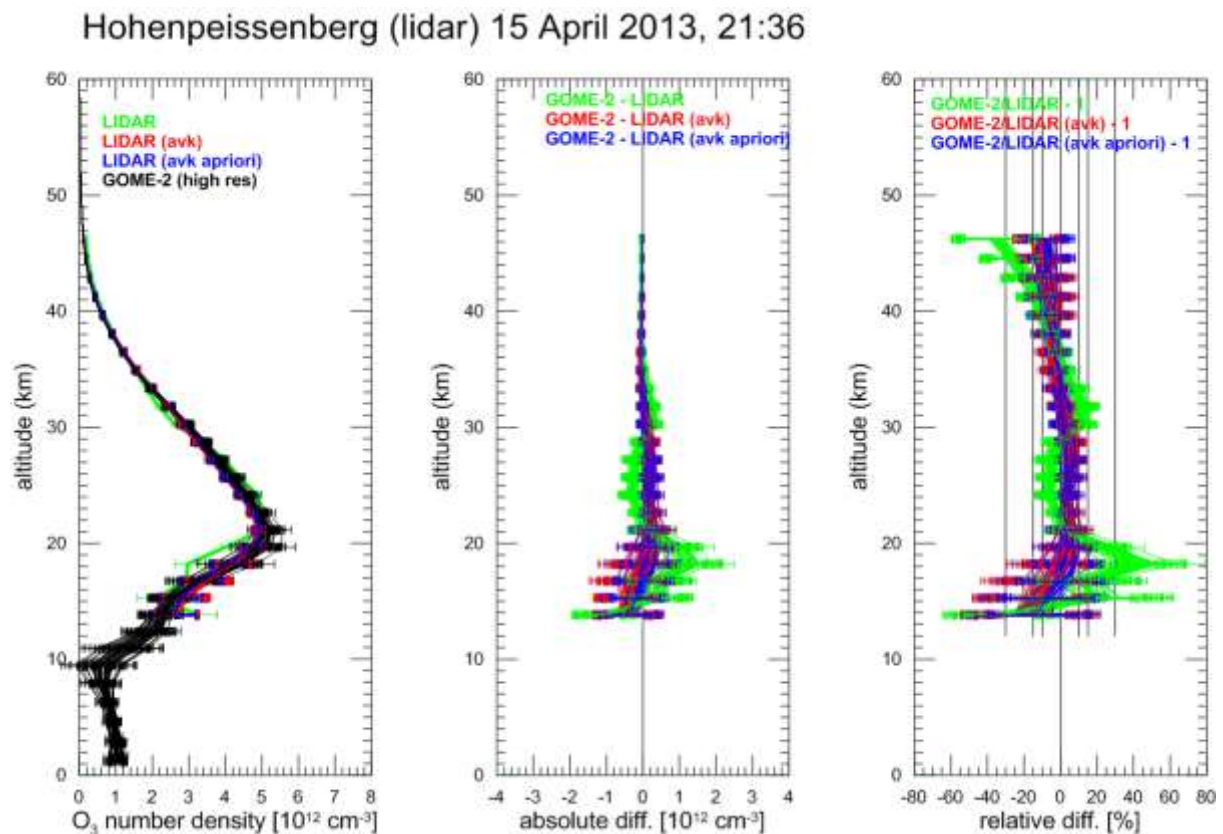


Figure 3.4: Example for the comparison of a lidar profile at Hohenpeissenberg, Germany, (green X_{ref} , red X_{avk} , blue $X_{avk, apriori}$) with the matching GOME-2 Metop-B high resolution profiles (black). Left panel: Profiles. Middle panel: Absolute differences. Right panel: Relative differences. Note that the GOME-2 layer altitudes and averaging kernels vary slightly from profile to profile. This results in small differences in the smoothed lidar profiles. Error bars (1σ) are from the reported measurement uncertainties for GOME-2 and lidar. The vertical lines at $\pm 30\%$, $\pm 15\%$, and $\pm 10\%$ in the right panel are the threshold, target, and optimum accuracies specified for the GOME-2 product.

3.6 Results

Validation a GOME-2 Metop-C ozone profile products:

This summary contains validation results for the GOME-2C high resolution (HR) ozone profile products, retrieved by the Ozone Profile Retrieval Algorithm (OPERA) at KNMI. The validation period covers February 2019 (the start of ozone profiles from GOME-2 on Metop-C) to December 2019 (after which time ground-based reference profiles become sparse).

To report the quality of GOME-2 ozone profile products in a very condensed way, the statistics for the different output levels of GOME-2 can be reduced to two layers: Lower Stratosphere (up to an altitude of 30 km) and Upper Stratosphere (above 30 km, up to 50 or 60 km). Table 3.2 shows the definition of the height ranges for lower and upper stratosphere for different latitude belts used in this report.

Table 3.2: Definition of the ranges in km for lower and higher stratosphere for the different latitude belts.

	Lower Stratosphere	Upper Stratosphere
Polar Region	12 km – 30 km	30 km – 50 km
Mid-Latitudes	14 km – 30 km	30 km – 50 km
Tropical Region	18 km – 30 km	30 km – 50 km

The validation for the lower stratosphere is made using ground-based ozonesonde data as a reference. For the upper stratosphere, ground-based lidar and microwave data are used as reference.

Relative differences (Eq. 1) are calculated against the ground-based reference data. Usually these are also convolved with the averaging kernels, including the a-priori contribution (Smoothed ground-based):

$$\frac{(\text{GOME-2} - \text{Smoothed ground-based}) * 100}{\text{Smoothed ground-based}} \quad (1)$$

Table 3.3 summarizes the overall difference between GOME-2C ozone profiles and ground-based reference profiles for the time period from February 2019 to December 2019, for the lower and upper stratosphere. Tropospheric ozone is discussed earlier in this report. The statistics for the lower stratosphere are obtained by KMI, the statistics for the upper stratosphere by DWD.

Table 3.3: Absolute Differences (AD), Relative Differences (RD) and standard deviation (STDEV) of GOME-2C HR ozone profile products versus ground-based reference profiles for lower and upper stratosphere and different latitude belts. Results are for the time period February 2019 – December 2019.

	GOME-2C HR					
	Lower Stratosphere			Upper Stratosphere		
	AD	RD	STDEV	AD	RD	STDEV
	(DU)	(%)	(%)	(DU)	(%)	(%)
Northern Polar Region	-8.2	-3.6	7.3	-6.3	-11,2	10,0
Northern Mid-Latitudes	-5.8	-2.2	8.4	-1,9	-2.5	8.8
Tropical Region	2.9	2.7	4.8	-7.9	-11,7	5.4
Southern Mid-Latitudes	-2.0	0.5	9.0			
Southern Polar Region	0.0	0.4	20.2	-	-	-

*The relative difference statistics are derived as a weighted average over the lower- and upper stratospheric ozone profile levels. The absolute differences however are integrated over respectively the lower- and upper stratospheric ozone profile levels.

The optimal goal (10% accuracy) stated in the GOME-2 ozone profile ATBD is met in both lower and upper stratosphere for nearly all belts under consideration. Figure 3.5 presents more details on the good overall agreement between GOME-2 ozone profiles from Metop-C (as well as -A and -B) and ground-based data from lidar and MWR. In Figure 3.5, for Metop-A and B, only data with improved degradation correction (time period 12/2018 to 06/2019) are shown. Clearly, GOME-2C performs very similar to (degradation corrected) GOME-2A and GOME-2B. Generally, GOME-2C ozone profiles lie well inside the optimal/target accuracy zone of $\pm 10\%$ / $\pm 15\%$ difference to the ground-based profiles.

The scatter plots in Figure 3.6 and Figure 3.7 demonstrate that ozone from GOME-2C and from reference ground-based MWR and lidars correlate well over a fairly wide range of ozone values and for altitudes between 15 and 50 km. As expected, the large natural variability of ozone in the lower stratosphere (below 25 km) results in more scatter, quite visible in the top-most rows of the four sub-panels in Fig. Figure 3.6 and Figure 3.7. In Figure 3.5, the same larger variability is reflected in the increased error bars below 22 km (particularly in the right panel of Figure 3.5).

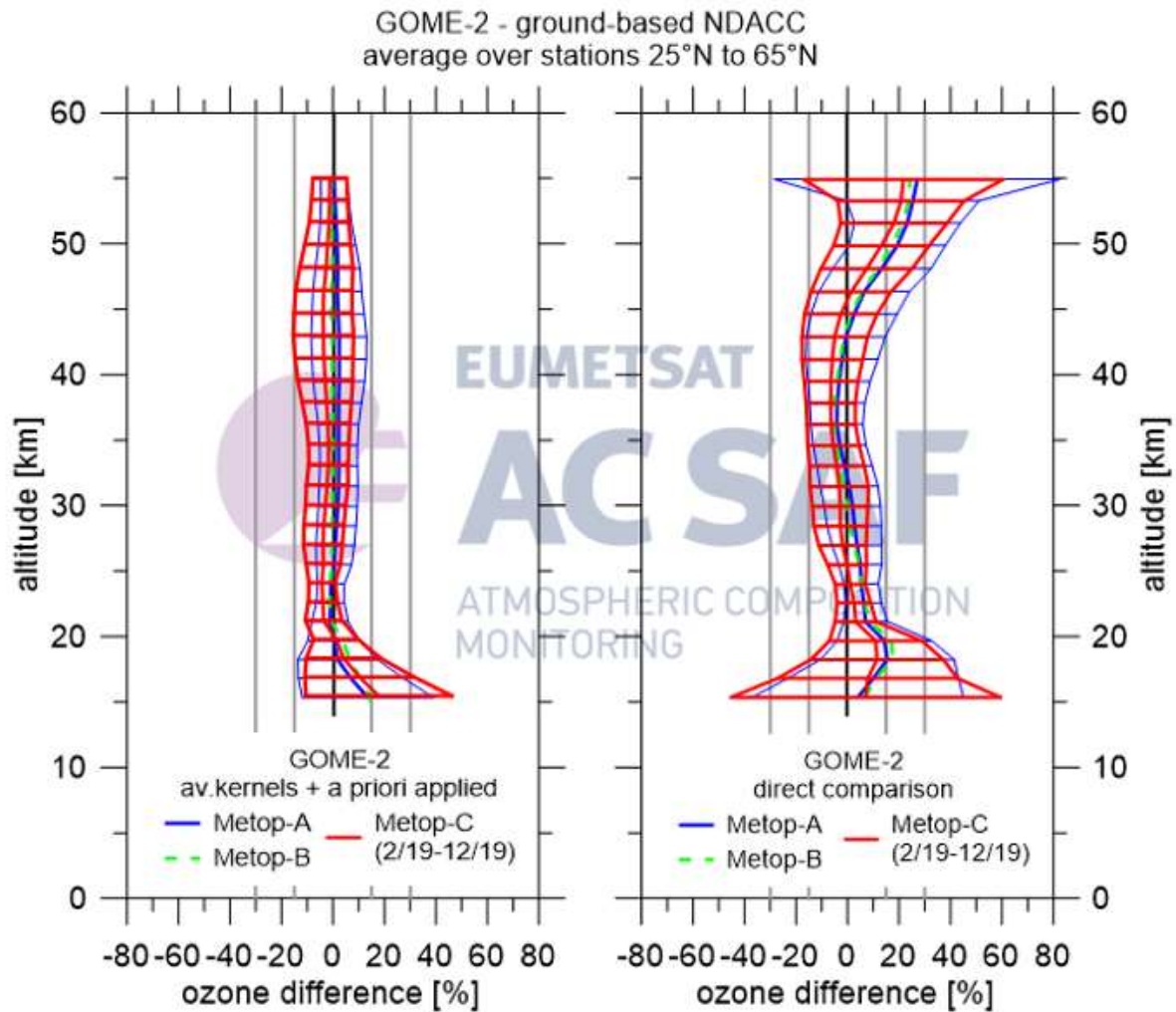


Figure 3.5: Average difference between GOME-2 MetopA/B/C ozone profiles and ground-based reference profiles from NDACC lidars and MWR in the 65°N to 25°N latitude belt (stations Hohenpeißenberg, Bern, Payerne, Haute-Provence and Table Mountain). Left panel: GOME-2 averaging kernels and a-priori contribution applied to the ground-based profiles. Right panel: direct comparison with no changes to the ground-based profiles. For GOME-2A and -2B only data from the period 12/2018 to 12/2019 are considered, when the improved GOME degradation correction was used in the operational KNMI retrieval. Error bars give ± 1 standard deviation of the differences.

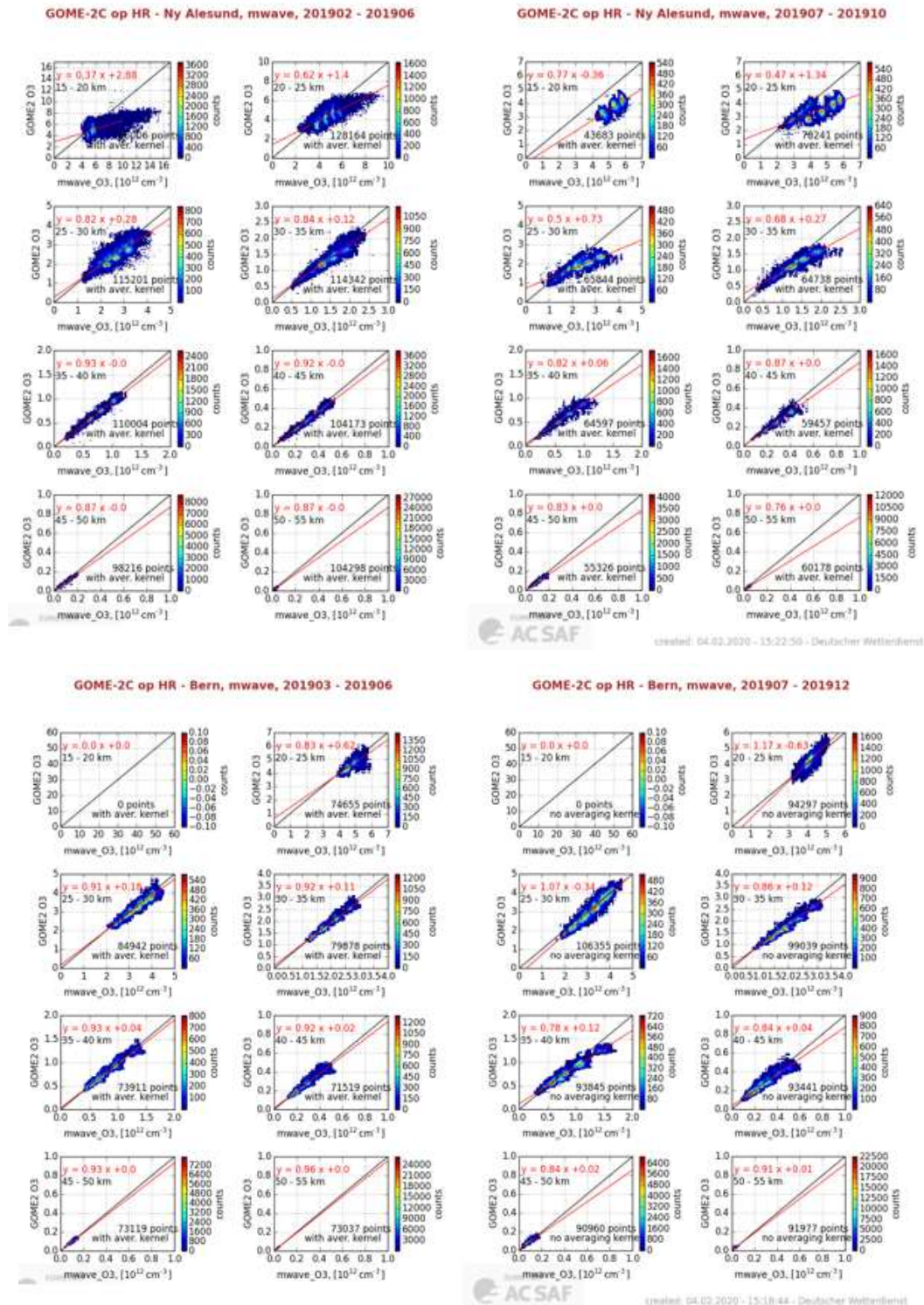


Figure 3.6: Scatter plot of GOME-2 Metop-C ozone versus NDACC ground-based ozone (GOME-2 kernels and a-priori applied), for different altitude ranges. For the MWRs at Ny-Ålesund (top panels) and Bern (lower panels).

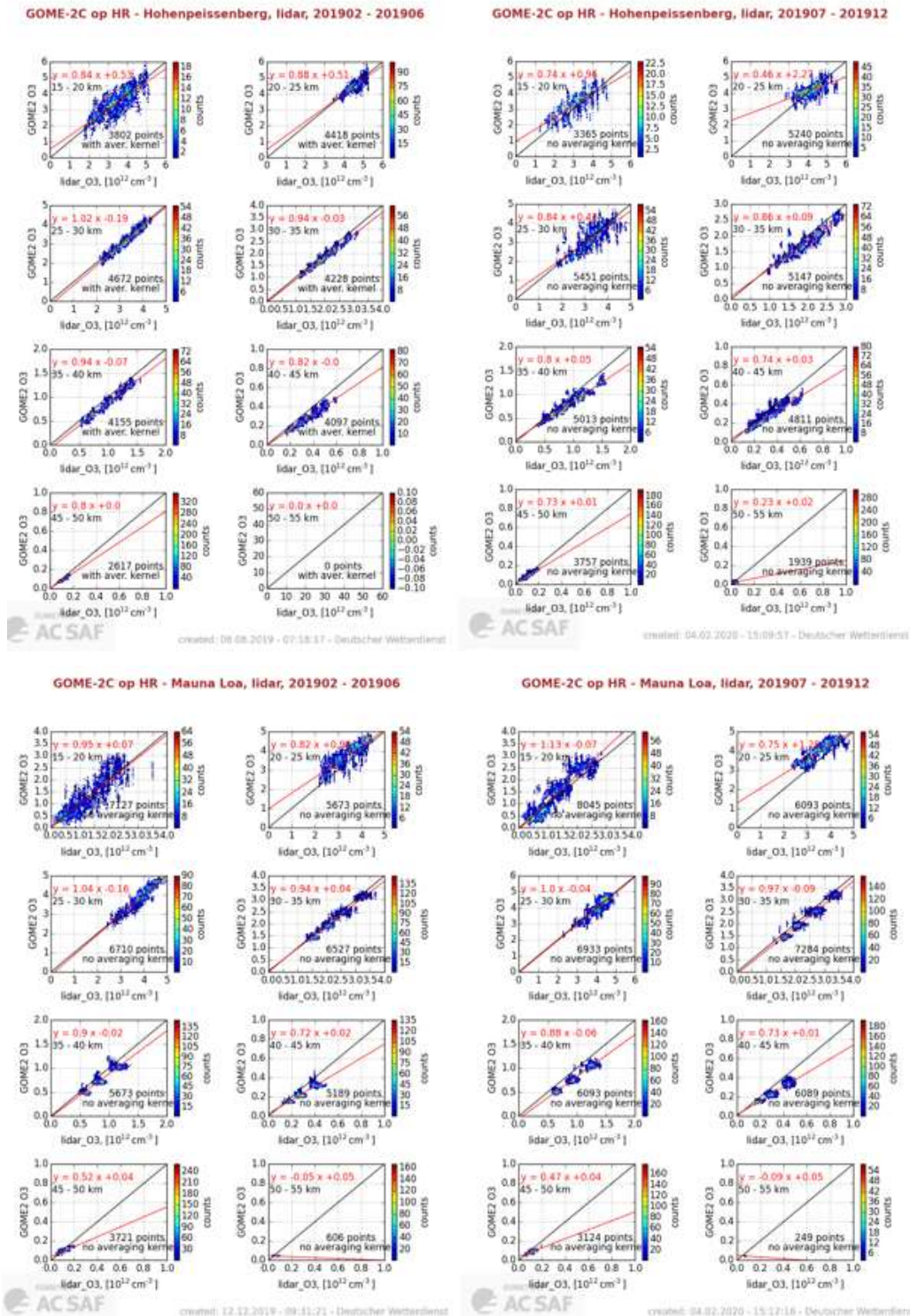


Figure 3.7: Scatter plot of GOME-2 Metop-C ozone versus NDACC ground-based ozone (GOME-2 kernels and a-priori applied), for different altitude ranges. For the the lidars at Hohenpeissenberg (top panels) and Mauna Loa (bottom panels).

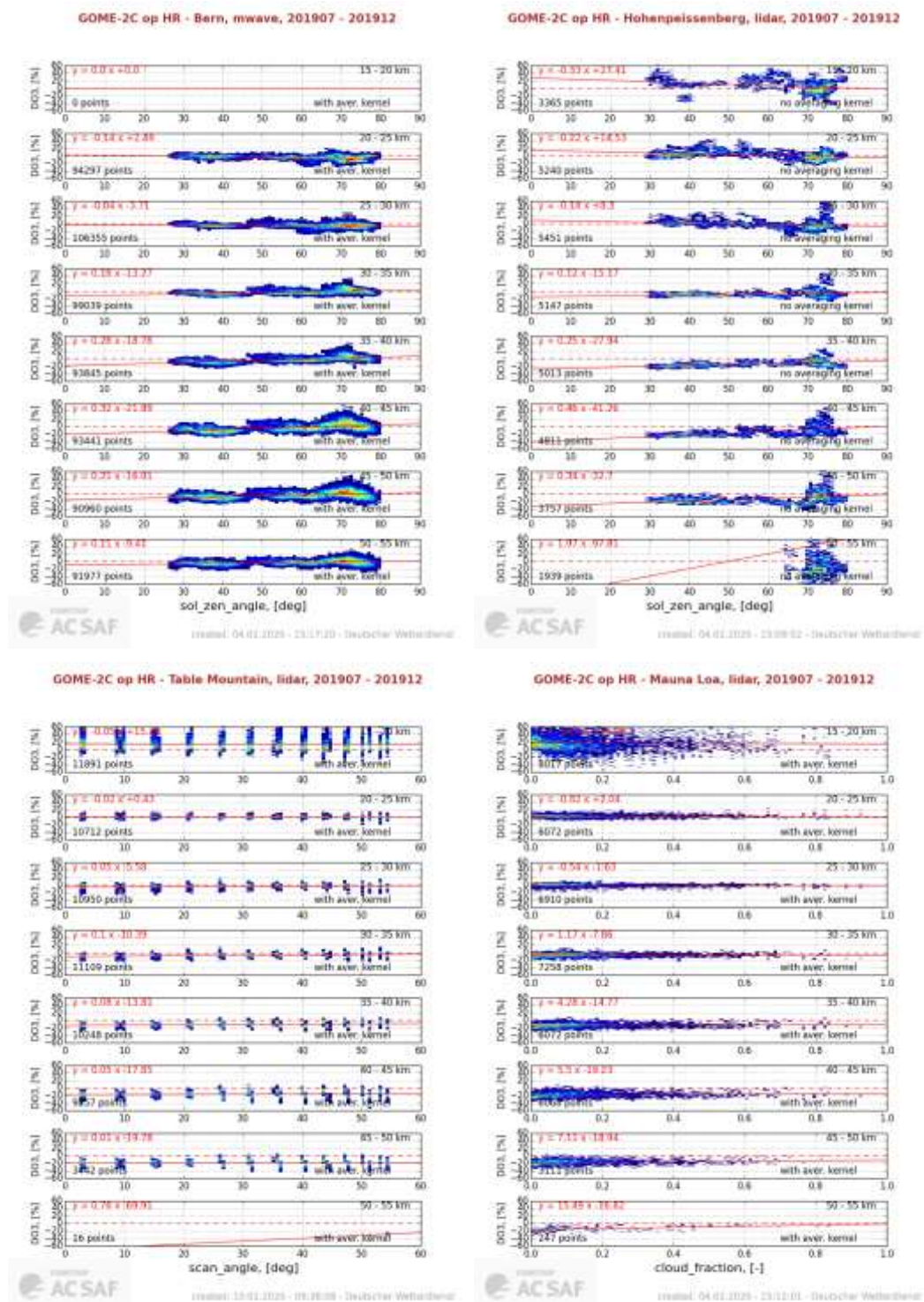


Figure 3.8: Scatter plot of ozone differences GOME-2 Metop-C – ground-based versus solar zenith angle for different altitudes at Bern (top left) and Hohenpeissenberg (top right); versus scan angle at Table Mountain (bottom left) and versus cloud fraction at Mauna Loa (bottom right). Most comparisons show little or no systematic dependency.

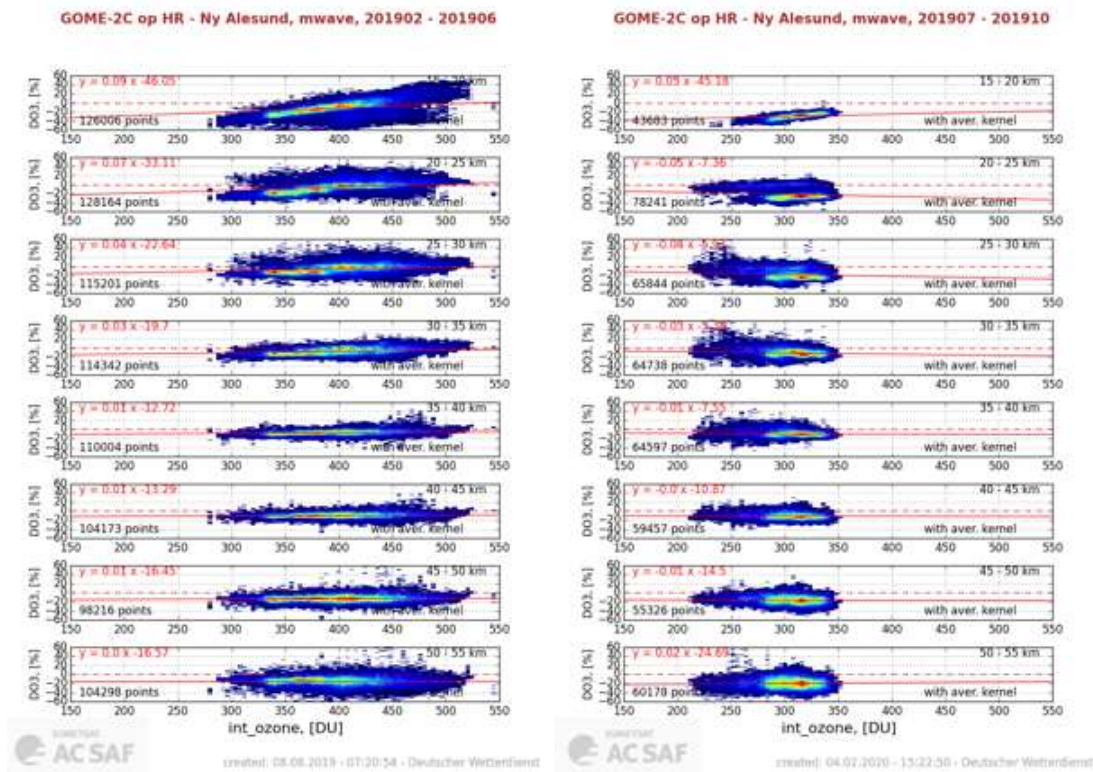


Figure 3.9: Examples of scatter plot of GOME-2 Metop-C - ground-based ozone differences versus total ozone column for the Ny-Ålesund MWR, which, in the lower stratosphere, might show some dependency on total column ozone. The comparison shows less variation with total ozone column.

Exemplary results on the correlation of differences between GOME-2C ozone and ground-based MWR and lidar ozone (GOME-2C – ground-based) are presented in Figure 3.8 and Figure 3.9. Based on the limited period of data available at this point (February 2019 to December 2019), it appears that GOME-2C – ground-based ozone differences do not vary significantly with solar zenith angle, cloud fraction, scan angle, or temporal or spatial distance between satellite and ground-based measurement. At most altitudes there is also no indication for a significant variation with total ozone column. The only exception is the lower stratosphere at higher latitudes, where data from Ny-Alesund and Lauder indicate that below 25 km GOME-2 tends to underestimate ozone when the total ozone column is low, and tends to overestimate ozone when the total ozone column is high. It remains to be seen if this effect persists when longer timeseries (a year or more of GOME-2C data) become available. However, a related annual cycle variation has been observed with GOME-2A and –B ozone profile data in the past.

Overall, these initial validation results show that GOME-2C ozone profiles are of good quality. In the stratosphere, they fulfill the $\pm 10\%$ optimal accuracy goal over a wide range of conditions, and the $\pm 15\%$ target accuracy under almost all conditions. GOME-2C ozone profiles are, at this

early stage of the mission, comparable to or better than GOME-2B and GOME-2A ozone profiles during their first years.

More detailed ozone profile validation results are available on the AC-SAF validation website at: http://acsaf.physics.auth.gr/eumetsat/ozone_profiles/, where results for MetOp-C have already been uploaded and will be published soon.

4. GOME-2/MetOp-C ozone integrated profiles validation using ground-based measurements

4.1 Dataset description

4.1.1 GOME-2/MetOp-C data

The GOME-2/MetOp-C (hereafter GOME-2C) integrated ozone profiles were produced by the same algorithm and methodology that is described in the “Vertical Ozone Profile and Tropospheric Ozone Column Products” ATBD¹. The only difference in the retrieval of the product for GOME-2C with regard to GOME-2/MetOp-A and GOME-2/MetOp-B (hereafter GOME-2A and GOME-2B) integrated ozone profiles, is that no degradation correction is applied due to the length of the time period of available data. The GOME-2C integrated ozone profile dataset available for validation spans the time period from February to December 2019.

In this report, the GOME-2C integrated profile was also compared to GOME-2C total ozone column product processed with the GDP4.9 algorithm.

4.1.2 Ground-based data

The ground-based database used for this validation report consists of archived Brewer and Dobson total ozone data that are downloaded from the World Ozone and Ultraviolet Radiation Data Centre (<http://www.woudc.org>). WOUDC is one of the World Data Centers which are part of the Global Atmosphere Watch (GAW) program of the World Meteorological Organization (WMO). These data are quality controlled, first by each station and secondly by WOUDC.

For the quality of the reference ground-based data used for the validation of the GOME-2C integrated ozone profiles product, updated information were extracted from recent inter-comparisons and calibration records. This continuously updated selection of ground-based measurements has already been used numerous times in the validation and analysis of global total ozone records such as the inter-comparison between the OMI/Aura TOMS and OMI/Aura DOAS algorithms (Balis et al., 2007a), the validation of ten years of GOME/ERS-2 ozone record (Balis et al., 2007b), the validation of the updated version of the OMI/Aura TOMS algorithm (Antón et al., 2009), the GOME-2/Metop-A validation (Loyola et al., 2011; Koukouli et al., 2012), the GOME-2/Metop-B validation (Hao et al., 2014), the evaluation of the

¹ https://acsaf.org/docs/atbd/Algorithm_Theoretical_Basis_Document_NHP_OHP_O3Tropo_Nov_2018.pdf

European Space Agency's Ozone Climate Change Initiative project (O3-CCI) TOCs (Koukouli et al., 2015, Garane et al., 2018) and the validation of the TROPOMI/S5P total ozone products (Garane et al., 2019). In all the aforementioned publications, LAP/AUTH assumes the leading role in the validation efforts.

In this report we use for the comparisons archived data for the period February to December 2019, depending on the availability of data for each individual station. Most stations upload their data to the WODC database two to four months after observation, which is the reason for the limited availability of data, especially for the southern hemisphere. The WODC stations considered for the comparisons are listed in Tables A.1 and A.2 (Appendix 1) and they are also spatially depicted in Figure 4.1. In Figure 4.2 the distribution of the co-locations of the ground-based measurements in space in time are showed.

In the comparison plots and statistics presented in this report, only the direct sun observations provided by the Brewers and Dobsons are utilized for the computation of the percentage differences between satellite and co-located (in space and in time) ground-based measurements, since they are considered of higher accuracy than all the other types of ground-based observations. Finally, only northern hemisphere Brewer ground-based stations are considered, because the number of stations in the southern hemisphere is very limited and they are mainly located in Antarctica.

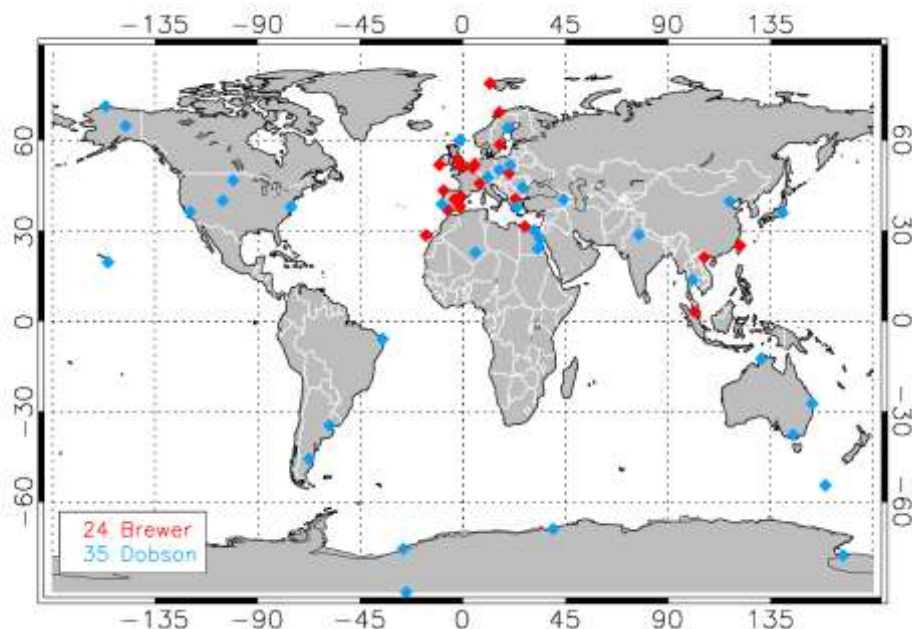


Figure 4.1: Spatial distribution of the Brewer and Dobson ground-based stations used for the comparisons.

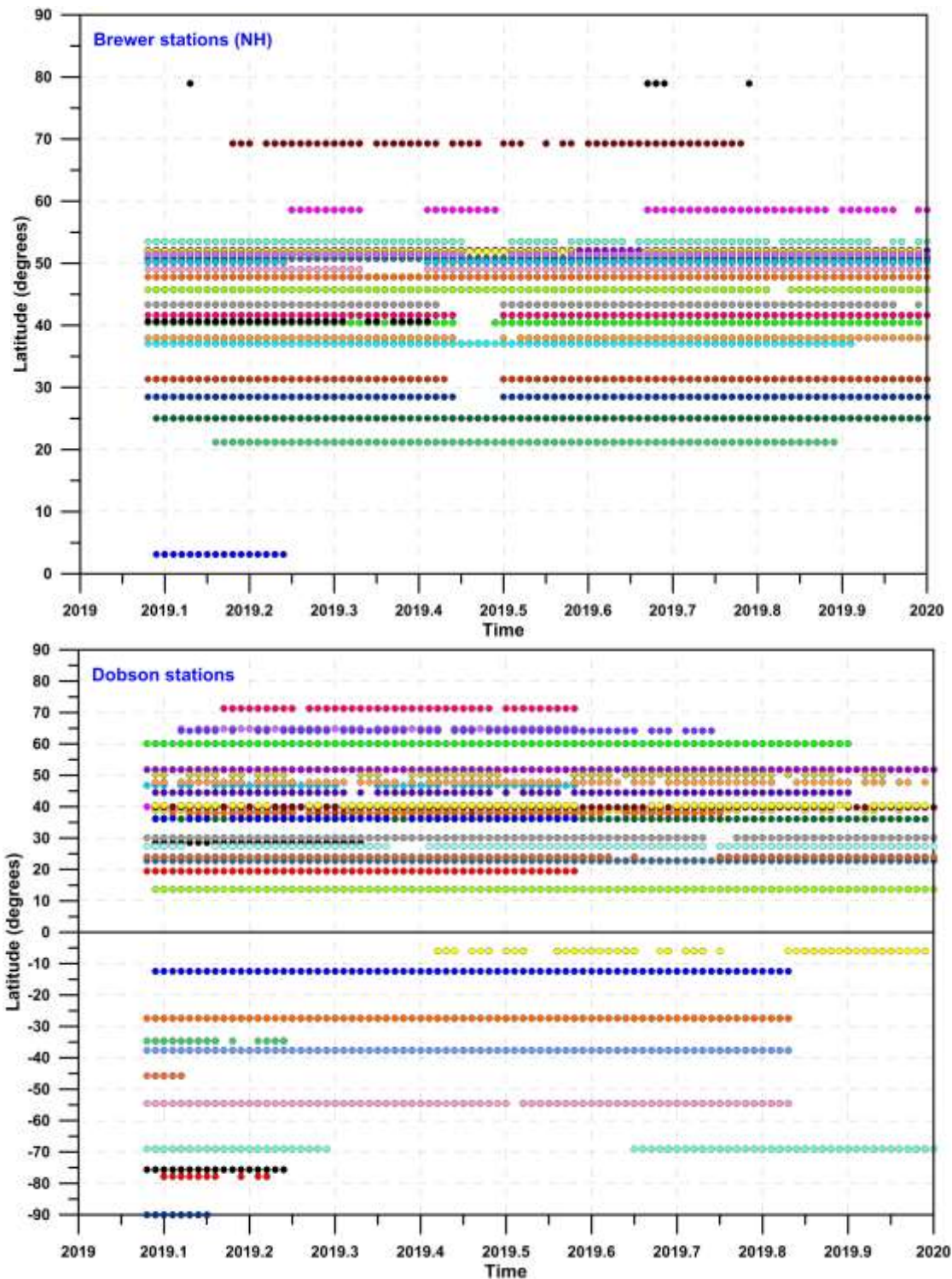


Figure 4.2: Spatial and temporal representation of the co-location data used for the validation with ground-based measurements (upper panel: Brewer, lower panel: Dobson) for the time period from February to December 2019.

4.1.3 GOME2/MetOp-A and GOME2/MetOp-B data

To further assess the quality of the GOME-2C integrated ozone profiles product, it is also compared to the respective products that were retrieved from GOME-2A and GOME-2B vertical ozone profile measurements. The algorithms for the retrieval of the three integrated ozone profile products are the same, except for the degradation correction, which was not applied to GOME-2C. Additional information for the ozone profiles retrieval algorithms are given in Figure 4.2.

For this validation report, only the temporally common co-locations between the three sensors are used to achieve the comparability between the datasets.

4.2 Validation of GOME-2C integrated ozone profiles

In this section, the archived and quality-controlled Dobson and Brewer daily total ozone measurements downloaded from WOUDC, for the period from February to December 2019, are used as ground-truth for the validation of GOME-2C integrated ozone profiles. The datasets of the three satellite sensors are temporally and spatially co-located to ground-based measurements using the following co-location criteria:

- the satellite and daily ground-based total ozone measurements must correspond to the same day, and
- the maximum search radius between the ground-based stations and the centre coordinates of the satellite pixel is set to 150 km. The spatially closest satellite observation is paired with the ground-based station's daily-mean measurement.

The pairs of co-located satellite and daily-mean ground-based measurements are used to calculate their percentage difference by the simple formula:

$$Diff (\%) = \frac{(satellite - ground)}{ground} \%$$

The datasets of percentage differences are then filtered:

- for solar zenith angle (SZA), which is limited up to 83°, because the mean percentage differences of the co-locations with SZA above 83° were higher than -10 %. The number of co-locations affected by this filtering criterion is ~ 1.3 % of the total.
- for latitude, which was limited up to 85° S, because the mean percentage differences of the co-locations with latitude above 85° S were higher than + 20 %. The number of co-locations affected by this filtering criterion is below 0.5% of the total.

The monthly means that are shown in the respective time-series plots are calculated by averaging the total number of available co-locations per month. Furthermore, the error bars in the following plots (where they are shown) stand for the 1σ standard deviation of the means.

Figure 4.3 shows the time series of the monthly mean percentage differences between GOME-2C and the co-located (in space and in time) ground-based measurements. Concerning the GOME-2C comparisons to Dobson in the northern hemisphere, the mean relative bias of the percentage differences was found to be about $+0.1 \pm 0.8 \%$, while compared to Brewer, GOME-2C has a mean bias about $-0.4 \pm 0.7 \%$. The respective mean standard deviation of the available monthly means is 2.6 - 3.1 %, depending on the ground-based instrument type, which is equal to or lower than the other two sensors' mean standard deviations. In the southern hemisphere, the GOME-2C mean bias is $-1.3 \pm 1.1 \%$, but it has a greater mean standard deviation (4.1 %) than in the northern hemisphere, which is mostly due to the limited availability of the ground-based measurements in this part of the globe. The slightly enhanced seasonality of the GOME-2C/Dobson comparisons is an expected feature due to the well-known dependency of the Dobson measurements on effective temperature (see Koukouli et al., 2016). Finally, panel (d) shows a scatter plot, where the good overall agreement (correlation coefficient = 0.970) of the GOME-2C integrated ozone profile to the ground-based TOC measurements from Dobson instruments, is shown. The respective correlation coefficient for the Brewer comparisons is 0.980, resulting from nearly 4000 co-locations.

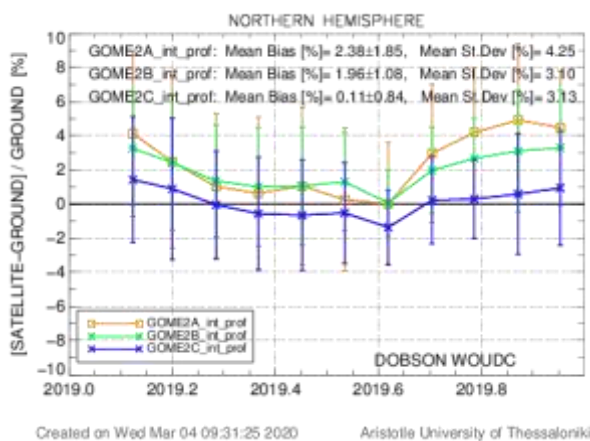
As for the consistency between the three sensors, it is very clear that, besides the difference in mean relative bias which goes up to 1.5 – 2%, with GOME-2A and GOME-2B reporting higher integrated ozone values than GOME-2C, they agree very well, capturing the same seasonal pattern in the percentage differences to ground-based measurements. GOME-2C complies better with GOME-2B than GOME-2A, especially during the second half of the time-series.

In Figure 4.4 the percentage differences between the ozone integrated profile retrieved by the three sensors (GOME-2C, GOME-2B and GOME-2A) and the TOC measurements performed by Dobson (left panel) and Brewer (right panel) ground-based instruments, are averaged in 10° latitude bins and displayed versus latitude. As it follows from the figures, GOME-2C reports lower ozone values compared to GOME-2A and GOME-2B, mainly in the tropics and the middle latitudes of both hemispheres. GOME-2A and GOME-2B agree very well regardless the latitude of the co-locations. The agreement of GOME-2C to the other two sensors is better in the northern hemisphere, where the difference is $\sim 2 \%$, decreasing to $\sim 0.5\%$ above 60°N . In the southern hemisphere (Dobson comparisons only) the difference of GOME-2C compared to the other two sensors is $\sim 3\%$ for the co-locations within $0^\circ - 40^\circ\text{S}$, it increases to 5% in the latitude bin $40^\circ\text{S} - 50^\circ\text{S}$ and it becomes much smaller above 50°S .

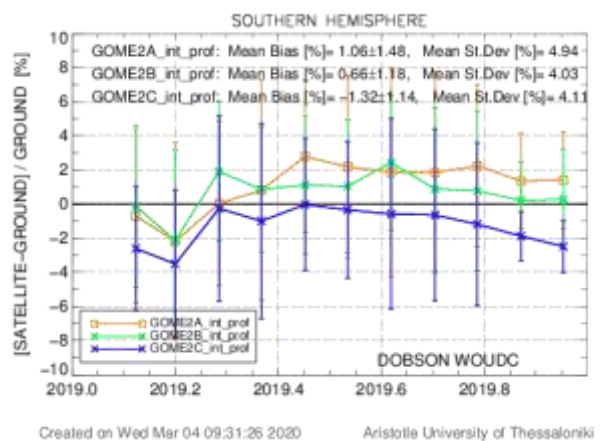
As for the dependency of the GOME-2C percentage differences on solar zenith angle (SZA), in Figure 4.5 it is seen that the Dobson comparisons below 80° have a negligible bias, up to $\pm 1\%$. Above 80° the dependency on SZA is enhanced but the respective number of co-locations is limited and come from the latitude bin -70°S to -80°S . The dependency on SZA is less pronounced for the Brewer comparisons, which come from the northern hemisphere stations only. The underestimation of $\sim 1.5 - 2 \%$, compared to the other two sensors for measurements

with SZAs that span 35°-65°, is well-noticed here as well, but the patterns of the dependency for the three sensors is very similar for moderate SZAs.

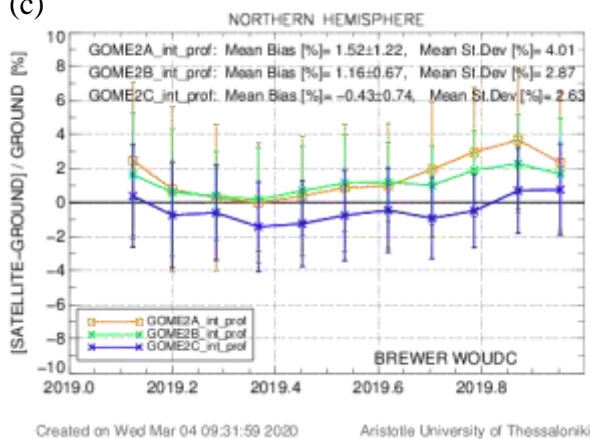
(a)



(b)



(c)



(d)

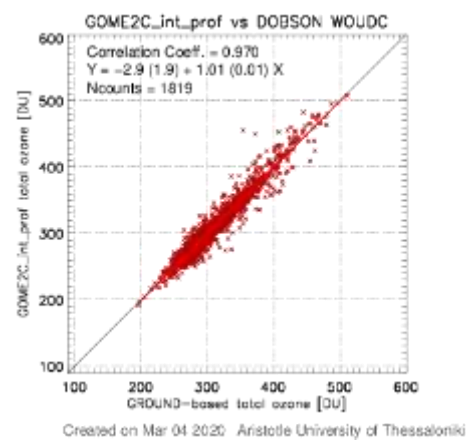


Figure 4.3: Panels (a) and (b): Time series of the monthly mean percentage differences between three sensors and Dobson ground-based measurements, for the NH (panel a) and the SH (panel b). The blue line and symbols show the GOME-2C comparisons, the green line and symbols show the GOME-2B comparisons and the orange line and symbols show the GOME-2A comparisons, for the same time period. Panel (c): the same as in panels (a) and (b), but for comparisons to Brewer measurements. Panel (d): the scatter plot of the GOME-2C and Dobson co-located measurements.

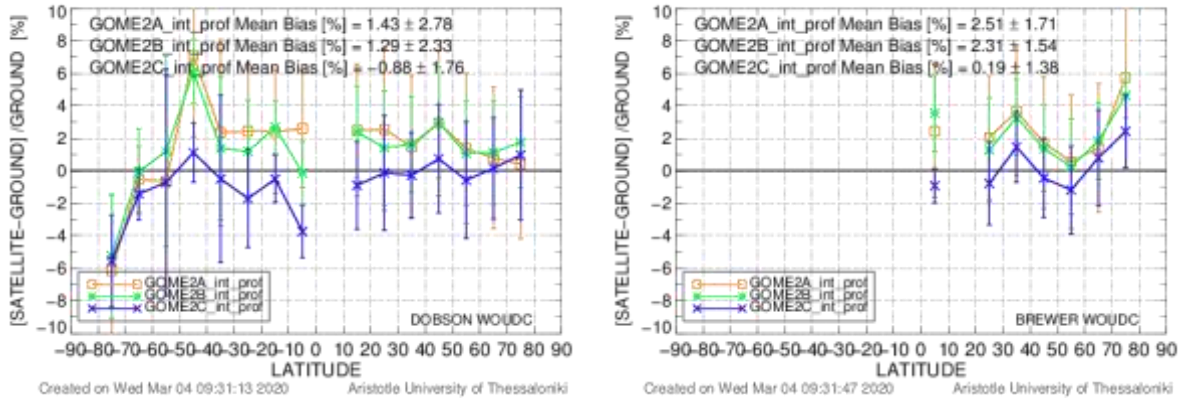


Figure 4.4: The latitudinal dependency of the percentage differences between the ozone integrated profile retrieved by the three sensors (GOME-2C, GOME-2B and GOME-2A) and the TOC measurements performed by Dobson (left panel) and Brewer (right panel) ground-based instruments.

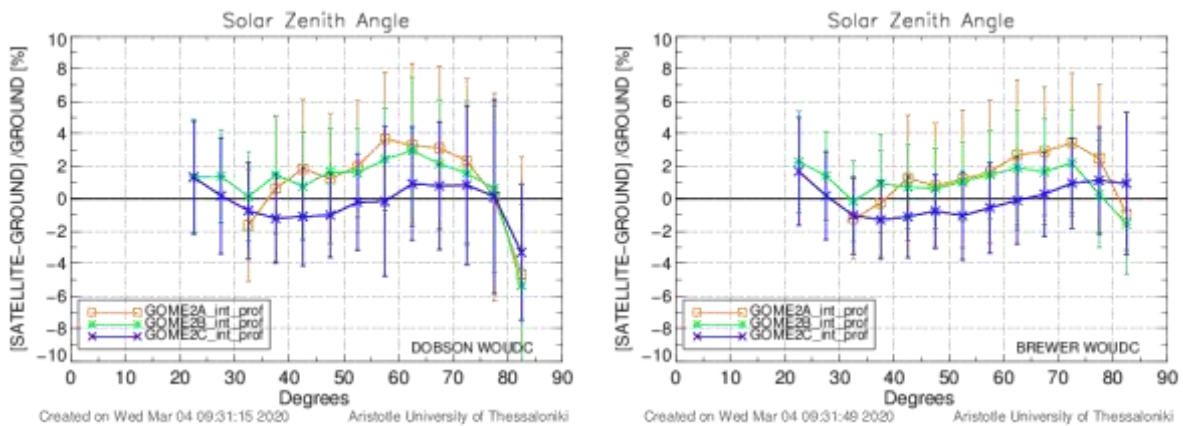


Figure 4.5: The dependency of the percentage differences on solar zenith angle. Left panel: the Dobson comparisons, right panel: the Brewer comparisons.

It is worth mentioning that according to the Product Requirements Document², the accuracy requirements for the GOME-2 Metop-A, -B and -C Total Ozone product are 4% for SZAs < 80° and 6% for SZAs > 80°. In the GOME-2C GDP4.9 total ozone validation report (Garane et al., 2020), it is shown that the respective accuracy that resulted from the analysis of 6 months

² Product Requirements Document, Issue 1.5, SAF/AC/FMI/RQ/PRD/001, Issue 1.5, D. Hovila, S. Hassinen, P. Valks, J., S. Kiemle, O. Tuinder, H. Joench-Soerensen, June 2019

of GOME-2C data (Febr. – July 2019) is well within these target values, being less than 3.7% for SZAs < 80° and less than 4.7% for SZAs > 80°. As it emerges from the same analysis for the GOME-2C integrated ozone profile product, the respective accuracy for SZAs < 80° is 3.7% and 4.2% for SZAs > 80°, well within the requirements, which proves that the integrated ozone profile is of similar quality to the (soon to be) operational product of GOME-2C TOC.

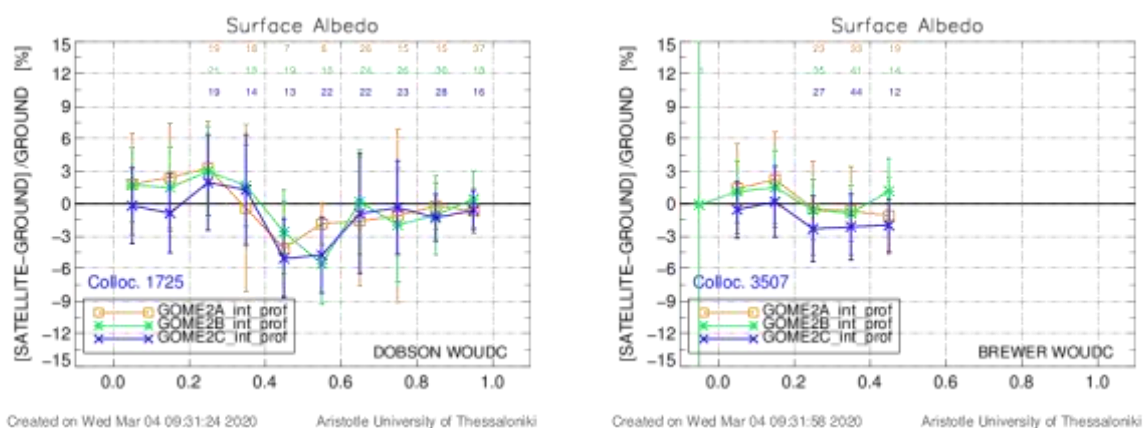


Figure 4.6: The dependency of the percentage differences on surface albedo for the Dobson (left panel) and the Brewer comparisons (right panel).

An additional interesting feature that was seen during this validation exercise, is the dependency of the percentage differences on surface albedo (Figure 4.6). The left panel includes the Dobson comparisons and the right panel averages the Brewer comparisons from the northern hemisphere only. Even though the majority of the co-locations³ in both cases correspond to measurements with surface albedo values 0 - 0.2, it is noticed that for surface albedo values between 0.4 and 0.6, the Dobson comparisons reveal a “U” shape dependency, which is also seen, but less pronounced, in the Brewer comparisons for surface albedos above 0.2. This indicates that the surface albedo parameter used in the retrieval algorithm should be further investigated.

Finally, no dependency on cloud parameters (not shown here), such as cloud fraction and cloud top pressure was seen.

³ Numbers on the upper part of the figures appear only if the number of co-locations in each averaging bin is below 5% of the total number of available co-locations.

4.3 Conclusions from the GOME-2C integrated ozone profile validation

The GOME-2C integrated ozone vertical profile was validated using ground-based daily measurements from Dobson and Brewer instruments, downloaded from WOUDC. The product under validation was also compared to the temporally and spatially co-located measurements from GOME-2A and GOME-2B, to further assess its consistency to their results. The validation results can be summarized to the following points:

- The comparisons of all three sensors had to be filtered for latitude. Their co-locations with Dobson ground-based measurements with latitude greater than 85° S had a mean percentage difference of $\sim +20\%$. This indicates that there is an issue with the products' retrieval algorithm in the Southern high latitudes that should be studied and resolved.
- Likewise, the comparisons with $SZA > 83^{\circ}$ had to be excluded, because their $\sim -10\%$ mean bias introduced a lot of noise in the measurements and their statistics.
- The statistical analysis (mean bias in $\% \pm$ mean standard deviation in $\%$) of the GOME-2C comparisons to co-located (in space and in time) Dobson and Brewer ground-based measurements is shown in Table 4.1, where it can be seen that the integrated ozone profile product agrees very well (difference up to $\pm 1\%$) with the ground-based data. Overall, GOME-2C reports lower integrated ozone vertical profile values by $\sim 1.5 - 2\%$ compared to the other two sensors used for this analysis.
- To further support this conclusion, the comparison of the GOME-2C integrated ozone profile product to the GOME-2C total ozone product processed with the GDP4.9 algorithm, is seen in Figure 4.7 for the Dobson comparisons only, where the underestimation of GOME-2C integrated profile w.r.t. GDP4.9 by 1% in the northern hemisphere and 2% in the southern hemisphere, is obvious. The respective underestimation for the Brewer comparisons (not shown here) is 1.1%.
- As it results from Table 4.1, the mean standard deviation of GOME-2C integrated profiles' comparisons is almost the same to GOME-2B (2.5 – 3 %), while GOME-2A shows a more enhanced variability ($\sim 4\%$).
- The seasonality of the GOME-2C measurements cannot be thoroughly studied since less than one year of data are available. Yet still, Figure 4.3 shows that GOME-2C has already a very similar seasonality pattern to GOME-2B.
- The latitudinal analysis of the comparisons showed that GOME-2C reports lower values of integrated ozone profile compared to GOME-2A and GOME-2B, mainly in the tropics and the middle latitudes of both hemispheres. The consistency between the three sensors is better towards the poles.
- The dependency of the comparisons on SZA showed very similar features for the three sensors. The $\sim 1.5\%$ underestimation of GOME-2C was prominent for $35^{\circ} < SZAs < 65^{\circ}$, where the number of co-locations is larger.

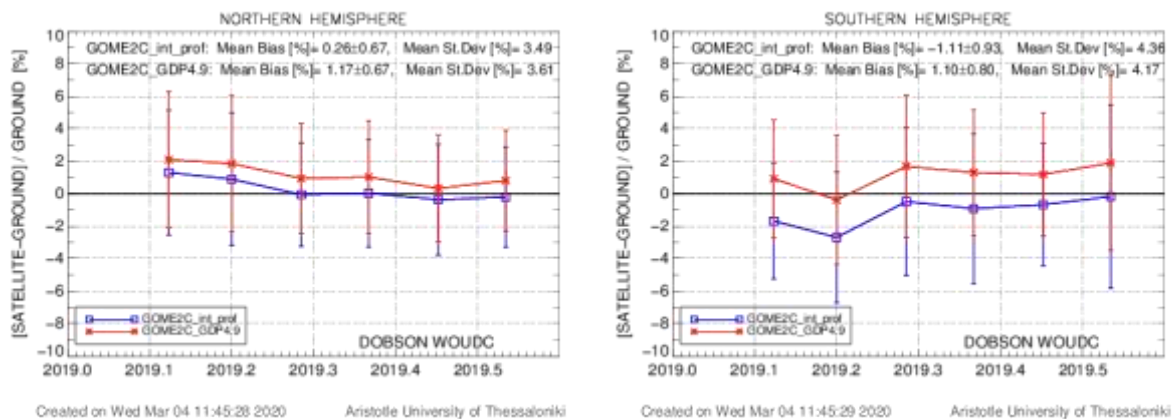


Figure 4.7: The time series of the percentage differences between Dobson measurements and GOME-2C integrated ozone profiles (blue line and symbols) and GOME-2C total ozone column processed with GDP4.9 (red line and symbols), for the northern (left panel) and the southern (right panel) hemisphere .

Table 4.1: The statistical analysis (mean bias in % ± mean standard deviation in %) of the comparisons of GOME-2C, GOME-2B and GOME-2A to Brewer (up) Dobson (down) ground-based measurements for the time period February – December 2019.

BREWER (NH)	GOME-2C	GOME-2B	GOME-2A
Overall averaging	-0.5 ± 2.7	+1.1 ± 2.9	+1.4 ± 4.2
Time series (NH) averaging	-0.4 ± 2.6	+1.2 ± 2.9	+1.5 ± 4.0
Latitudinal averaging	+0.2 ± 2.3	+2.3 ± 2.5	+2.5 ± 4.2
DOBSON (NH & SH)	GOME-2C	GOME-2B	GOME-2A
Overall averaging	-0.3 ± 3.6	+1.5 ± 3.7	+1.7 ± 4.8
Time series (NH) averaging	+0.1 ± 3.1	+1.9 ± 3.1	+2.4 ± 4.2
Time series (SH) averaging	-1.3 ± 4.1	+0.7 ± 4.0	+1.1 ± 4.9
Latitudinal averaging	-0.9 ± 3.2	+1.3 ± 3.2	+1.4 ± 4.5

- Other influence parameters and their effect on the comparisons were also studied, but no alarming dependencies were found, except for a dependency on surface albedo for a rather small part (~ 2% of the co-locations) of the available dataset.

In conclusion, the validation of the GOME-2C integrated ozone profile shows that this product is of very good quality. It is in excellent agreement with the co-located ground-based measurements, and even though it reports lower values than GOME-2A and GOME-2B by about 1.5 - 2 %, the patterns of its dependency on many important parameters such as latitude, solar zenith angle, etc, are very consistent to GOME-2A and they are in even better agreement to GOME-2B. Finally, GOME-2C's variability is lower than the other two sensors, indicating that during the first 11 months of its operation it is very stable and reliable.

5. General conclusions

The GOME-2C vertical ozone profile product was validated against data from measurements with ozonesonde, microwave and lidar. For the first time, also Dobson and Brewer measurements were used to validate the quality of the integrated ozone profile product. Both products are also compared with the current operational ozone profile products, derived from GOME-2A and GOME-2B.

It is shown that the optimal goal (10% accuracy) stated in the GOME-2 ozone profile [ATBD](#) is met in both lower and upper stratosphere for nearly all belts under consideration for the GOME-2C product.

The validation results for the GOME-2A/2B/2C integrated ozone profile confirm that this product is of very good quality. It is in excellent agreement with the co-located ground-based measurements.

LAP/AUTH is announcing the upgrade of the [AC SAF Ozone Validation & Quality Assessment web pages which have undergone substantial maintenance and have been moved to a newer, faster and more stable host server](#). The ACSAF validation webpages currently present the validation results of GOME-2/MetopA and GOME-2/MetopB GDP4.8 [near real-time](#) and [offline](#) Total Ozone Data, following the availability of the ground-based observations. Furthermore, the [high resolution Ozone Profile](#) validation comparative plots are hosted here, while the links to the [Trace Gas](#) and [UV](#) validation pages remain the same. After the GOME2/MetopC ORR is complete, relevant fields that permit access to the Total Ozone and Ozone Profiles validation results will automatically appear.

6. Acknowledgement

The ozonesonde data was made available by WOUDC (<http://www.woudc.org>), the SHADOZ network (<http://croc.gsfc.nasa.gov/shadoz/>) and the NILU's Atmospheric Database for Interactive Retrieval (NADIR) at Norsk Institutt for Luftforskning (NILU) (<http://www.nilu.no/nadir/>). Lidar and microwave radiometer ozone profiles were retrieved from the Network for the Detection of Atmospheric Composition Change (NDACC) (<http://www.ndsc.ncep.noaa.gov/>) and the NILU Atmospheric Database for Interactive Retrieval (NADIR) at Norsk Institutt for Luftforskning (NILU). The total ozone ground-based data was made available by WOUDC (<http://www.woudc.org>).

7. References

- Antón, M., Loyola, D., López, M., et al.: Comparison of GOME-2/MetOpA total ozone data with Brewer spectroradiometer data over the Iberian Peninsula, *Annales Geophysicae*, 27, 1377–1386, DOI:10.5194/angeo-27-1377-2009, 2009.
- Balis, D., Kroon, M., Koukouli, M. E., et al.: Validation of Ozone Monitoring Instrument total ozone column measurements using Brewer and Dobson spectrophotometer ground-based observations, *J. Geophys. Res.*, 112, D24S46, doi:10.1029/2007JD008796, 2007a
- Balis, D., Lambert, J.-C., Van Roozendael, M., Spurr, R., Loyola, D., Livschitz, Y., Valks, P., Amiridis, V., Gerard, P., Granville, J., Zehner, C.: Ten years of GOME/ERS2 total ozone data—The new GOME data processor (GDP) version 4: 2. Ground-based validation and comparisons with TOMS V7/V8, *J. Geophys. Res.*, 112, D07307, doi:10.1029/2005JD006376, 2007b
- Loyola, D., Koukouli, M., Valks, P., Balis, D., Hao, N., Van Roozendael, M., Spurr, R., Zimmer, W., Kiemle, S., Lerot, C., and Lambert, J.-C.: The GOME-2 Total Column Ozone Product: Retrieval Algorithm and Ground-Based Validation, *J. Geophys. Res.*, 116, D07302, doi:10.1029/2010JD014675, 2011.
- Boyd, I. S., A. D. Parrish, L. Froidevaux, T. von Clarmann, E. Kyrölä, J. M. Russell III, and J. M. Zawodny (2007), Ground-based microwave ozone radiometer measurements compared with Aura-MLS v2.2 and other instruments at two Network for Detection of Atmospheric Composition Change sites, *J. Geophys. Res.*, 112, D24S33, doi:10.1029/2007JD008720.
- Delcloo A., and L. Kins (2009, 2012): Ozone SAF Validation report.
- Delcloo A. and K. Kreher (2013): Ozone SAF Validation report.
- Garane, K., Lerot, C., Coldewey-Egbers, M., Verhoelst, T., Koukouli, M. E., Zyrichidou, I., Balis, D. S., Danckaert, T., Goutail, F., Granville, J., Hubert, D., Keppens, A., Lambert, J.-C., Loyola, D., Pommereau, J.-P., Van Roozendael, M., and Zehner, C.: Quality assessment of the Ozone_cci Climate Research Data Package (release 2017) – Part 1: Ground-based validation of total ozone column data products, *Atmos. Meas. Tech.*, 11, 1385–1402, <https://doi.org/10.5194/amt-11-1385-2018>, 2018.

Garane, K., Koukouli, M.-E., Verhoelst, T., Lerot, C., Heue, K.-P., Fioletov, V., Balis, D., Bais, A., Bazureau, A., Dehn, A., Goutail, F., Granville, J., Griffin, D., Hubert, D., Keppens, A., Lambert, J.-C., Loyola, D., McLinden, C., Pazmino, A., Pommereau, J.-P., Redondas, A., Romahn, F., Valks, P., Van Roozendael, M., Xu, J., Zehner, C., Zerefos, C., and Zimmer, W.: TROPOMI/S5P total ozone column data: global ground-based validation and consistency with other satellite missions, *Atmos. Meas. Tech.*, 12, 5263–5287, <https://doi.org/10.5194/amt-12-5263-2019>, 2019.

Garane K., M.E. Koukouli, D. Balis, K.P. Heue, P. Valks: ACSAF GOME2/MetopC Total Ozone Validation Report, SAF/AC/AUTH/VR/O3, 2020

Godin S., G. Mégie, J. Pelon, Systematic Lidar Measurements of the Stratospheric Ozone vertical Distribution, *Geophys. Res. Lett.*, 16, 547-550, 1989.

Hao, N., Koukouli, M. E., Inness, A., Valks, P., Loyola, D. G., Zimmer, W., Balis, D. S., Zyrichidou, I., Van Roozendael, M., Lerot, C., and Spurr, R. J. D.: GOME-2 total ozone columns from MetOp-A/MetOp-B and assimilation in the MACC system, *Atmos. Meas. Tech.*, 7, 2937-2951, <https://doi.org/10.5194/amt-7-2937-2014>, 2014

Hocke, K.; N. Kämpfer, D. Ruffieux, L. Froidevaux, A. Parrish, I. Boyd, T. von Clarmann, T. Steck, Y.M. Timofeyev, A.V. Polyakov, E. Kyrölä, Comparison and synergy of stratospheric ozone measurements by satellite limb sounders and the ground-based microwave radiometer SOMORA, *Atmos. Chem. Phys.*, 7, 4117-4131, 2007

Keckhut, P.; I. S. McDermid, D. Swart, T. J. McGee, S. Pal, S. Godin-Beekmann, A. Adriani, J. Barnes, H. Bencherif, H. Claude, G. Fiocco, G. Hansen, A. Hauchecorne, T. Leblanc, C. H.

Koukouli, M. E., Balis, D. S., Loyola, D., Valks, P., Zimmer, W., Hao, N., Lambert, J.-C., Van Roozendael, M., Lerot, C., and Spurr, R. J. D.: Geophysical validation and long-term consistency between GOME-2/MetOp-A total ozone column and measurements from the sensors GOME/ERS-2, SCIAMACHY/ENVISAT and OMI/Aura, *Atmos. Meas. Tech.*, 5, 2169-2181, <https://doi.org/10.5194/amt-5-2169-2012>, 2012.

Koukouli, M. E., Lerot, C., Granville, J., Goutail, F., Lambert, J.-C., Pommereau, J.-P., Balis, D., Zyrichidou, I., Van Roozendael, M., Coldewey-Egbers, M., Loyola, D., Labow, G., Frith, S., Spurr, R., and Zehner, C.: Evaluating a new homogeneous total ozone climate data record from GOME/ERS-2, SCIAMACHY/Envisat, and GOME-2/MetOp-A, *J. Geophys. Res.*, 120, 12296–12312, <https://doi.org/10.1002/2015JD023699>, 2015

Lee, G. Mégie, H. Nakane and R. Neuber, Review of ozone and temperature lidar validations performed within the framework of the Network for the Detection of Stratospheric Change, *J. Environ. Monit.*, 6, 721 – 733, doi:10.1039/B404256E, 2004.

Leblanc, T., and I. S. McDermid, Stratospheric Ozone Climatology From Lidar Measurements at Table Mountain (34.4°N, 117.7°W) and Mauna Loa (19.5°N, 155.6°W), *J. Geophysical Research*, 105, 14,613-14,623, 2000.

Lobsiger E., K.F. Künzi and H.U. Dütsch, Comparison of stratospheric ozone profiles retrieved from microwave-radiometer and Dobson-spectrometer data, *J. Atm. and Terr. Phys.*, 46, 799-806, 1984.

Parrish, A., R.L. de Zafra, P.M. Solomon, and J.W. Barrett, A ground-based technique for millimeter wave spectroscopic observations of stratospheric trace constituents, *Radio Sci.*, 23, 106-118, 1988.

Rodgers C.D., Characterization and Error Analysis of Profiles Retrieved from Remote Sounding Measurements, *J. Geophys. Res.*, 95, 5587-5595, 1990.

Sterling, C. W., Johnson, B. J., Oltmans, S. J., Smit, H. G. J., Jordan, A. F., Cullis, P. D., Hall, E. G., Thompson, A. M., and Witte, J. C.: Homogenizing and estimating the uncertainty in NOAA's long-term vertical ozone profile records measured with the electrochemical concentration cell ozonesonde, *Atmos. Meas. Tech.*, 11, 3661–3687, <https://doi.org/10.5194/amt-11-3661-2018>, 2018.

Steinbrecht W., et al. (2006), Long-term evolution of upper stratospheric ozone at selected stations of the Network for the Detection of Stratospheric Change (NDSC), *J. Geophys. Res.*, 111, D10308, doi:10.1029/2005J

Thompson, A. M., Witte, J. C., Sterling, C., Jordan, A., Johnson, B. J., Oltmans, S. J., ... Thiongo, K. (2017). First reprocessing of Southern Hemisphere Additional Ozonesondes (SHADOZ) ozone profiles (1998–2016): 2. Comparisons with satellites and ground-based instruments. *Journal of Geophysical Research: Atmospheres*, 122. <https://doi.org/10.1002/2017JD027406>

8. APPENDIX I

Table A. 1: List of Dobson ground-based stations used for the comparisons

STATION ID	NAME	COUNTRY	LONGITUDE (degrees)	LATITUDE (degrees)	Last day of available measurement
2	Tamanrasset	Algeria	5.51	22.78	31-DEC-2019
10	New Delhi	India	77.17	28.63	30-APR-2019
14	Tateno	Japan	140.13	36.05	27-DEC-2019
19	Bismarck	USA	-100.75	46.76	31-JUL-2019
27	Brisbane	Australia	153.08	-27.42	31-OCT-2019
29	Macquarie island	Australia	158.93	-54.49	31-OCT-2019
31	Mauna Loa	USA	-155.57	19.54	31-JUL-2019
43	Lerwick	UK	-1.18	60.13	25-NOV-2019
57	Halley Bay	Antarctica	-26.18	-75.62	30-MAR-2019
67	Boulder	USA	-105.26	39.99	28-JUL-2019
68	Belsk	Poland	20.79	51.84	31-DEC-2019
82	Lisbon	Portugal	-9.13	38.76	17-DEC-2019
84	Darwin	Australia	130.88	-12.42	31-OCT-2019
91	Buenos-aires	Argentina	-58.48	-34.59	31-MAR-2019
96	Hradec Kralove	Czech_Republic	15.83	50.18	11-DEC-2019

99	Hohenpeissenberg	Germany	11.01	47.80	30-DEC-2019
101	Syowa	Antarctica	39.58	-69.00	31-DEC-2019
105	Fairbanks	USA	-147.87	64.82	31-JUL-2019
107	Wallops island	USA	-75.46	37.94	31-JUL-2019
111	Amundsen-Scott	Antarctica	-24.80	-89.99	25-FEB-2019
152	Cairo	Egypt	31.28	30.08	31-DEC-2019
199	Barrow	USA	-156.61	71.32	31-JUL-2019
208	Shiangher	China	116.96	39.75	31-DEC-2019
216	Bangkok	Thailand	100.62	13.67	31-DEC-2019
219	Natal	Brazil	-35.20	-6.00	30-DEC-2019
226	Bucharest	Romania	26.13	44.48	26-NOV-2019
245	Aswan	Egypt	32.783	23.96	31-DEC-2019
253	Melbourne	Australia	144.83	-37.66	31-OCT-2019
268	Arrival Heights	Antarctica	166.66	-77.83	24-MAR-2019
284	Vindeln	Sweden	19.77	64.23	27-SEP-2019
293	Athens	Greece	23.73	37.98	30-SEP-2019
341	Hanford	USA	-119.63	36.32	31-JUL-2019
342	Comodoro Rivadavia	Argentina	-67.50	-45.78	14-FEB-2019
409	Hurghada	EGU	33.75	27.42	31-DEC-2019
410	Amberd	ARM	44.25	40.38	30-DEC-2019

Table A. 2: List of Brewer ground-based stations used for the comparisons.

STATION ID	NAME	COUNTRY	LONGITUDE (degrees)	LATITUDE (degrees)	Last day of available measurement
53	Uccle	Belgium	4.35	50.79	31-DEC-2019
89	Ny Alesund	Norway	11.92	78.92	18-OCT-2019
95	Taipei	Taiwan	121.48	25.02	31-DEC-2019
96	Hradec Kralove	Czech Republic	15.83	50.18	31-DEC-2019
99	Hohenpeissenberg	Germany	11.01	47.80	31-DEC-2019
213	El Arenosillo	Spain	-6.73	37.10	30-NOV-2019
261	Thessaloniki	Greece	22.96	40.63	31-MAY-2019
279	Norkoping	Sweden	16.15	58.58	31-DEC-2019
284	Vindeln	Sweden	19.76	64.23	15-NOV-2019
308	Madrid	Spain	-3.72	40.45	29-DEC-2019
316	Debilt	Netherlands	5.18	52.10	31-DEC-2019
318	Valentia	Ireland	-10.25	51.94	29-DEC-2019
322	Petaling Jaya	Malaysia	101.65	3.10	31-MAR-2019
330	Hanoi	Vietnam	105.80	21.20	23-NOV-2019
331	Poprad-Ganovce	Slovakia	20.32	49.03	31-DEC-2019
346	Murcia	Spain	-1.17	38.00	31-DEC-2019
352	Manchester	GBR	-2.23	53.47	31-DEC-2019
353	Reading	GBR	-0.94	51.44	31-DEC-2019
376	Mrsa_mtrouh	Egypt	27.22	31.33	31-DEC-2019
401	Santa Cruz	Spain	-16.25	28.47	31-DEC-2019
405	La Coruna	Spain	-8.47	43.33	27-DEC-2019
411	Zaragoza	ESP	-0.91	41.63	31-DEC-2019
476	Andoya	NOR	16.01	69.28	11-OCT-2019
479	Aosta	ITA	7.36	45.74	31-DEC-2019

Table A. 3: List of all ozonesonde stations used for the comparisons

STATION	Longitude	Latitude	Nr of profiles	Last day available ozonesonde
ASCENSION	-7.98	-14.42	7	20-Feb-19
BROADMEADOWS	-37.69	144.95	50	18-Dec-19
DEBILT	52.1	5.18	50	27-Dec-19
FIJI	-18.1	178.4	1	25-Jan-19
HILO	19.717	-155.083	9	28-Feb-19
HOHENPEISSENBERG	47.8	11.02	128	30-Dec-19
IRENE	-25.9	28.22	4	6-Mar-19
LAUDER	-45.045	169.684	31	25-Jul-19
LERWICK	60.14	-1.19	25	3-Jul-19
MACQUARIE_ISL	-54.5	158.94	47	31-Dec-19
NAIROBI	-1.27	36.8	9	28-Feb-19
NEUMEYER	-70.39	-8.15	55	24-Dec-19
NY-ALESUND	78.93	11.95	73	30-Dec-19
PARAMARIBO	5.81	-55.21	16	25-Jun-19
PAYERNE	46.817	6.95	33	29-Mar-19
SAMOA	-14.23	-170.56	2	28-Feb-19
SODANKYLA	67.3666	26.6297	19	17-Jun-19
SOUTH_POLE	-89.99	-24.8	19	30-Jul-19
TATENO-TSUKUBA	36.1	140.1	39	29-Nov-19
UCCLE	50.8	4.35	148	23-Dec-19
VALENTIA	51.93	-10.25	28	31-Dec-19

Table A. 4: List of all lidar and MWR stations used for the comparisons

STATION	Longitude	Latitude	Nr of profiles	Last day available measurement
Lidar:				
HOHENPEISSENBERG	47.8	11.02	95	23-Dec-19
MAUNALOA	19.54	155.58	119	31-Dec-19
OBS: HAUTE PROVECE	43.94	5,71	20	29-Mar-19
TABLE MOUNTAIN	34.4	117.7	195	20-Dec-19
MWR:				
BERN	46.95	7.45	1971	31-Dec-19
MAUNALOA	19.54	155.58	113	31-Aug-19
NY-ALESUND	78.93	11.95	1913	31-Oct-19
PAYERNE	46.82	6.95	228	21.-Sep-19